Universitá degli Studi di Napoli
"Federico II"
Facoltá di Ingegneria

Doctorate thesis in Electrical Engineering

Semi-Analytic Models for the Characterisation of Microstrips

Dario Assante

Tutor: Prof. Luigi Verolino
Coordinatore: Prof. Giovanni Miano

November 2005

To my parents

Contents

Acknowledgements

First of all, I have to thank my parents and my sister Grazia. They have always helped me, they have believed in me and always sustained me in the difficulties. What I have made of good in my life, I mainly owe it to them, and for this reason I devote them this thesis. I hope they can be proud of me.

I believe that the whole time I have devoted to realize this thesis has been subtracted to my love, Fabiola. My thought has been constantly turned to her when I have written this thesis. Apart from thanking her for the patience and the understanding, I have to apologize for all the time I haven't spent with her.

A special thank is for the prof. Verolino. I must thank him for everything he has taught me in these three years, in the job and in the life. All the results achieved in this thesis derive from his teachings.

I can't forget to thank Simone Falco for all the interesting discussions we had in these years on many arguments. It has always been a great help for me the possibility to discuss my ideas with him.

Finally, I have to thank the prof. Miano for all the support he gave me in these three year and for the outstanding activities he organized for the doctorate.

Chapter 1

An overview on the microstrips

1.1 The problems of interconnects in high frequency circuits

The performances of the integrated circuits in the range of the radio frequency (RF) strongly influence the versatility and the portability of the future electronic systems, especially for wireless communications. Considering the continuos request of a faster ability for the systems to transmit informations and an even increasing need of bandwidth for several applications, united to the demand to reduce the weight and the costs of the chips, the necessity of robust and more efficient RF circuits is destined to increase.

Actually the microwave integrated circuits (MMICs) are developed in the range of frequencies 10-100 GHz and they represent the base of the RF components used in great part of the wireless systems. With the recent introduction of the micro-electromechanical systems, new applications of the RF devices have been discovered. From a careful analysis of the daily activities, it has been evaluated that a medium family requires a transmission capability next to 100 Mbps, due to the transmission of different informative contents, from the vocal signal to the high resolution images. That requires a high bandwidth.

This request leads to more and more complex integrated circuits, able to reach high clock speeds. Within the technology of the semiconductors, the need to reach even higher frequencies has produced a considerable increase of the density of the components (transistors) and of the interconnections on a

	1997	2003	2006	2012
Chip size (mm^2)	300	430	520	750
Number of transistors (milions)	11	76	200	1400
Interconnect width (nm)	200	100	70	35
Total interconnect length (km)	2.16	2.84	5.14	24

Table 1.1: Increasing of the circuit density in the years

single chip, as it is deduced by the data presented in the following table 1.1.

From the previsions on the dimensions of the chips and the interconnections, it is evident the trend for the reduction of the size of the interconnects, realized on more levels, and the increase of their general length (24 Km in 2012 !). So the realization of efficient projects since the beginning will become fundamental.

Within the technology MOS, the density of the transistors per die can be reassumed through the figure 1.1. It can be found a value greater than 10^9 for the memories.

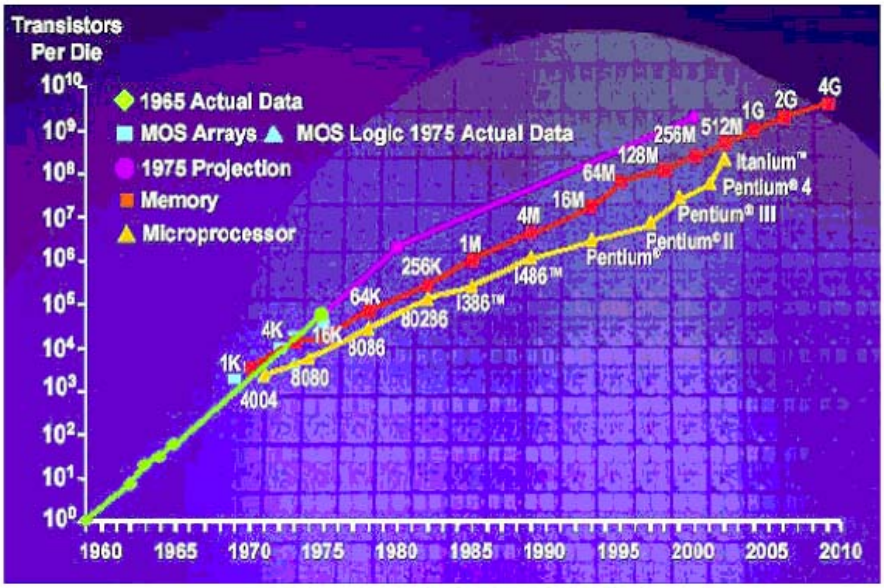

Figure 1.1: Evolution of the number of transistors used to realize some kind of circuits

The to need reach high frequencies and elevated transmission speeds has

accented some electromagnetic undesired phenomena that limit the electric performances of the integrated circuits and increase their vulnerability to noises and transmission error. The undesired phenomena may be crosstalk, ground bounce, bypass capacitors and inductors,..

In the integrated circuits, the degradation of the performances manifests itself through a greater delay in the transmission of the signals. The delay may be generated by the gates and by the interconnects. As the technology progresses, the gate delay tends to reduce, while the delay due to the interconnects increases, as shown in figure 1.2.

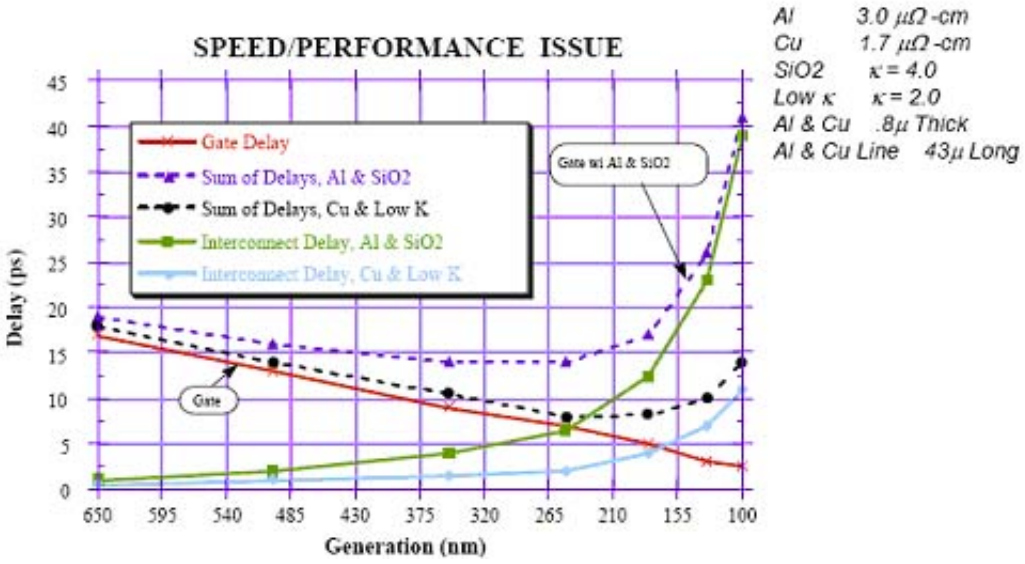

Figure 1.2: Gate delay and interconnect delay as function of the technology used to realize the circuits

The use of copper interconnects instead of the aluminium ones produces a smaller interconnect. Anyway, at the current state of the technology, the relevant limitation to the performance of the circuits is due to the interconnects.

Another problem related to the interconnects is the heating of the circuits. The density of the interconnections (m/cm^2), considering only the active ones on an integrated circuit, excluding the different levels, is strongly destined to grow (table 1.2).

Year	1997	2003	2006	2012
Chip size (mm^2)	300	430	520	750

Table 1.2: Density of the interconnects in the years

This growth of the length of the interconnections will bring to increase the resistances, the parasite capacitance and inductance of the metalizations, causing worse performances of the circuits as the dimensions are reduced. From some verifications it has been found that, for the 130 nm technology, the power dissipated by the interconnections results to be more than the 50

From all these reasons, the problem of the interconnects covers a fundamental and critical role in the project of high speed high performance RF circuits.

1.2 The role of the microstrips between the interconnects

Various types of transmission lines can be used to connect different circuits. In figure 1.3 most of the existing interconnects are shown.

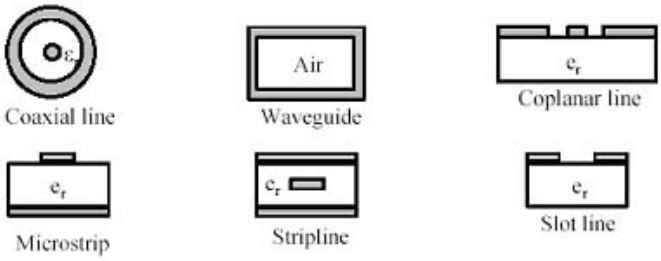

Figure 1.3: Different kind of interconnects

The planar transmission lines are one of the essential elements of the integrated circuits and the microwave printed circuits boards. The more used planar structure is the microstrip. It is a structure composed by a ground plane, a dielectric substrate and a conducting strip placed over it. Even if it's an open structure, the field is almost confined in the dielectric and it is propagated along the metalization. Such a structure has the great advantage to

be easily realizable with today's technologies and contributes to considerably decrease the dimensions of the circuits themselves.

Characteristic	Coaxial cable	Waveguide	Stripline	Microstrip
Losses	Medium	Low	High	High
Bandwidth	Medium	Great	Small	Small
Integration	Vary bad	Very bad	Good	Excellent
Volume and weigh	High	High	Medium	Low
Realization	Easy	Easy	Very Easy	Very Easy

Table 1.3: Main characteristics of the different kind of interconnects

1.3 Models for the analysis of microstrips

To analyse complex integrated circuit it's not possible to use an unique technique, but different approaches have to be used or different detail levels. Of course, in a structure containing several chips, components, interconnects, it's not possible to perform a full wave analysis of the whole structure, as it requires an almost infinite computational time. On the other hand, a full wave simulation can describe phenomenas that a lumped circuit neglects. The pyramid shown in figure 1.4 expresses a good compromise between different methods.

To describe single elements, such as interconnects, a full-wave analysis has to be adopted. As the complexity of the circuit grows, the analysis is always less accurate, since to the large network analysers used for the entire circuits. Anyway, the results obtained in a lower level are the base to perform the simulation at an higher level. For example, the results of a full-wave analysis are used to extract an equivalent circuit to use in the lumped element simulation.

The work performed in this thesis is located in the lower part of the pyramid. The objective is to furnish some methodologies for the accurate evaluation of the electromagnetic characteristics of a microstrip. The full-wave models proposed can be useful for the extraction of equivalent circuit parameters. From an analysis of the available models in literature, it is possible to find that some approximations are usually assumed to simplify the treatment.

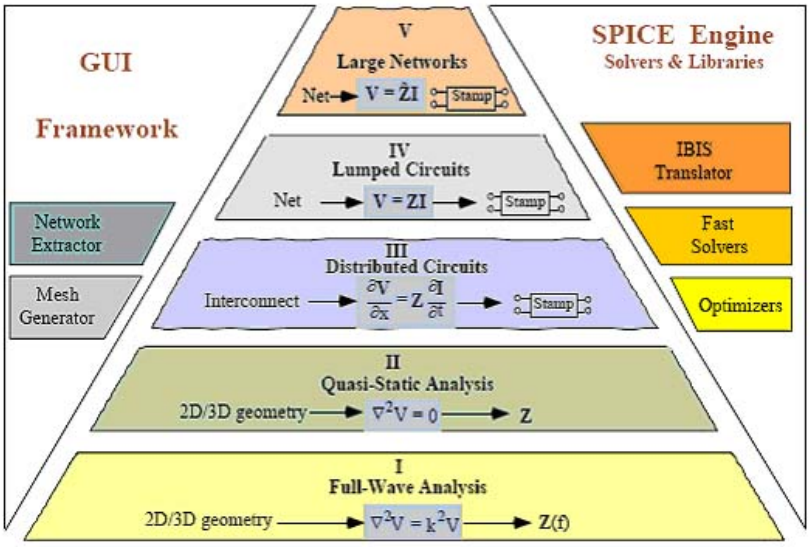

Figure 1.4: Different approaches to analyse integrated circuits

It can be observed that it is usual to neglect the conductive losses of the structure, that nevertheless result more and more remarkable with the increase of the density of the circuits. Besides, the existing models for the analysis of microstrips don't generally take into account the thickness of the structure, if not in a perturbative way. This thesis has the objective to propose some models that try to eliminate or however to reduce the approximation around the finite conductivity and the finite thickness of a microstrip.

Chapter 2

Single microstrip of infinitesimal thickness

2.1 Introduction

In this chapter, the behaviour of a single lossless microstrip of infinitesimal thickness will be examined. The objective of this study is to present the general method used for the solution of this kind of structures. The proposed method is based on an analysis of the structure in the spectral domain, which allows to reduce the problem to a system of dual integral equations. The system will be resolved using a representation in series of functions of Bessel (Neumann series). The geometry of the problem is shown in figure 2.1: a microstrip of infinitesimal thickness, width $2a$ indefinite along the z axis, over a substrate of relative electric permittivity ε_r and height d, located over a perfectly conducting ground plane.

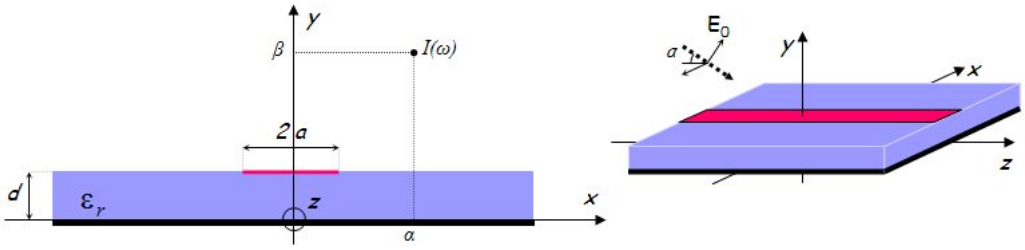

Figure 2.1: Geometry of the problem and sources

As forcing field we use either a plane wave, with the wave-number vector

$\vec{k}$ placed in the y-z plane, or a wire of current located in the point (α, k) and independent from the z variable.

2.2 A general solution for the electromagnetic field

In this section, the transverse components of the electromagnetic field is expressed as function of its longitudinal components, namely E_z and H_z. Then, a general expression of the longitudinal components will be found in the spectral domain. Let's start from Maxwell equations in the frequency domain, for an isotropic and homogeneous media:

$$\nabla \times \vec{E} = -j\omega\mu\vec{H} \tag{2.1}$$
$$\nabla \times \vec{H} = j\omega\varepsilon\tilde{\mathrm{E}} \tag{2.2}$$
$$\nabla \cdot \vec{E} = 0 \tag{2.3}$$
$$\nabla \cdot \vec{H} = 0 \tag{2.4}$$

It's possible to suppose a dependence from the variable z as:

$$\vec{E}(x, y, z) = \vec{e}(x, y)e^{-jk_z z} \tag{2.5}$$
$$\vec{H}(x, y, z) = \vec{h}(x, y)e^{-jk_z z} \tag{2.6}$$

So Maxwell equations become:

$$\nabla \times \vec{e} - jk_z\hat{z} \times \vec{e} = -j\omega\mu\vec{h} \tag{2.7}$$
$$\nabla \times \vec{h} - jk_z\hat{z} \times \vec{h} = j\omega\varepsilon\vec{e} \tag{2.8}$$
$$\nabla \cdot \vec{e} - jk_z\hat{z} \cdot \vec{e} = 0 \tag{2.9}$$
$$\nabla \cdot \vec{h} - jk_z\hat{z} \cdot \vec{h} = 0 \tag{2.10}$$

Dividing the electromagnetic field in a component along the z axis and in a component transverse to this direction, namely $\vec{e} = \vec{e}_t + e_z\hat{z}$ and $\vec{h} = \vec{h}_t + h_z\hat{z}$,

the equations (2.7) and (2.8) can be rewritten as follows:

$$\nabla \times \vec{e}_t + \nabla e_z \times \hat{z} - jk_z\hat{z} \times \vec{e}_t = -j\omega\mu\vec{h}_t - j\omega\mu h_z\hat{z} \tag{2.11}$$

$$\nabla \times \vec{h}_t + \nabla h_z \times \hat{z} - jk_z\hat{z} \times \vec{h}_t = j\omega\mu\vec{e}_t + j\omega\varepsilon e_z\hat{z} \tag{2.12}$$

Also the operator ∇ can be divided in a longitudinal and in a transverse component, that is:

$$\nabla = \nabla_t + \frac{\partial}{\partial z}\hat{z} \tag{2.13}$$

So the equations (2.11), (2.12), (2.9), (2.10) become:

$$\nabla_t \times \vec{e}_t + \nabla_t e_z \times \hat{z} - jk_z\hat{z} \times \vec{e}_t = -j\omega\mu\vec{h}_t - j\omega\mu h_z\hat{z} \tag{2.14}$$

$$\nabla_t \times \vec{h}_t + \nabla_t h_z \times \hat{z} - jk_z\hat{z} \times \vec{h}_t = j\omega\mu\vec{e}_t + j\omega\varepsilon e_z\hat{z} \tag{2.15}$$

$$\nabla_t \cdot \vec{e}_t - jk_z\hat{z} \cdot e_z = 0 \tag{2.16}$$

$$\nabla_t \cdot \vec{h}_t - jk_z\hat{z} \cdot h_z = 0 \tag{2.17}$$

From equations (2.14) and (2.15) it is possible to obtain the transverse components of the fields as function of the longitudinal ones. In particular, assuming $k = \omega\sqrt{\varepsilon\mu}$:

$$\vec{e}_t = -\frac{k^2}{k^2 - k_z^2}\frac{1}{j\omega\varepsilon}\left(\hat{z} \times \nabla_t h_z - \frac{k_z}{\omega\mu}\nabla_t e_z\right) \tag{2.18}$$

$$\vec{h}_t = \frac{k^2}{k^2 - k_z^2}\frac{1}{j\omega\mu}\left(\hat{z} \times \nabla_t e_z + \frac{k_z}{\omega\varepsilon}\nabla_t h_z\right) \tag{2.19}$$

or, more explicitly:

$$e_x = \frac{k^2}{k^2 - k_z^2}\frac{1}{j\omega\varepsilon}\left(\frac{k_z}{\omega\mu}\frac{\partial e_z}{\partial x} + \frac{\partial h_z}{\partial y}\right) \tag{2.20}$$

$$e_y = \frac{k^2}{k^2 - k_z^2}\frac{1}{j\omega\varepsilon}\left(\frac{k_z}{\omega\mu}\frac{\partial e_z}{\partial y} - \frac{\partial h_z}{\partial x}\right) \tag{2.21}$$

$$h_x = \frac{k^2}{k^2 - k_z^2}\frac{1}{j\omega\mu}\left(-\frac{\partial e_z}{\partial y} + \frac{k_z}{\omega\varepsilon}\frac{\partial h_z}{\partial x}\right) \tag{2.22}$$

$$h_y = \frac{k^2}{k^2 - k_z^2}\frac{1}{j\omega\mu}\left(-\frac{\partial e_z}{\partial x} + \frac{k_z}{\omega\varepsilon}\frac{\partial h_z}{\partial y}\right) \tag{2.23}$$

To the longitudinal components of the fields satisfy an Helmholtz equation, that can be obtained from the equations (2.16) and (2.17):

$$\left[\frac{\partial^2}{\partial x^2} + \frac{\partial^2}{\partial y^2} + \left(k^2 - k_z^2\right)\right] e_z = 0 \tag{2.24}$$

$$\left[\frac{\partial^2}{\partial x^2} + \frac{\partial^2}{\partial y^2} + \left(k^2 - k_z^2\right)\right] h_z = 0 \tag{2.25}$$

To solve these equations it is useful to introduce a spatial Fourier transform:

$$\tilde{E}_z(w, y) = \int_{-\infty}^{+\infty} e_z(x, y) e^{-jwx} dx \tag{2.26}$$

So the previous equations become:

$$\frac{\partial^2}{\partial y^2}\tilde{E}_z(w, y) + \left(k^2 - k_z^2 - w^2\right)\tilde{E}_z(w, y) = 0 \tag{2.27}$$

$$\frac{\partial^2}{\partial y^2}\tilde{H}_z(w, y) + \left(k^2 - k_z^2 - w^2\right)\tilde{H}_z(w, y) = 0 \tag{2.28}$$

Assuming $A(w) = \sqrt{k^2 - k_z^2 - w^2}$, the general solution of these equations is:

$$\tilde{E}_z(w, y) = C_1^E(w) e^{jAy} + C_2^E(w) e^{-jAy} \tag{2.29}$$

$$\tilde{H}_z(w, y) = C_1^H(w) e^{jAy} + C_2^H(w) e^{-jAy} \tag{2.30}$$

The constants C have to be found imposing the constrains of the problem.

2.3 Formulation of the problem in terms of currents

In the previous section, a general expression for the electromagnetic field, under some assumptions, has been found. The solution of the problem has to be found imposing the boundary conditions of the problem. Both in the dielectric and in the free space, the total electromagnetic field can be decomposed as a term due to the forcing field (E_0 and H_0), that already takes into account the presence of the dielectric and the ground plane, and in an unknown term due to the

current density induced on the microstrip.

$$\vec{E}_{TOT}(x,y) = \vec{E}_0(x,y) + \vec{E}(x,y) \tag{2.31}$$

$$\vec{H}_{TOT}(x,y) = \vec{H}_0(x,y) + \vec{H}(x,y) \tag{2.32}$$

Since the forcing field already satisfies the boundary conditions, the general expression developed in the previous section is used only to develop the unknown field. In future, all the fields will be marked with the subscript 1 in the dielectric and the subscript 2 in the free space. The following quantities are defined: $k_1 = \omega\sqrt{\epsilon_1\mu_0}$, $k_2 = \omega\sqrt{\epsilon_0\mu_0}$, $A_1 = \sqrt{k_1^2 - k_z^2 - w^2}$, $A_2 = \sqrt{k_2^2 - k_z^2 - w^2}$. Then, the unknown parts of the electromagnetic field can be expressed:

inside the dielectric

$$\tilde{E}_{1z}(w,y) = C_{11}^E(w)e^{jA_1y} + C_{12}^E(w)e^{-jA_1y} \tag{2.33}$$

$$\tilde{H}_{1z}(w,y) = C_{11}^H(w)e^{jA_1y} + C_{12}^H(w)e^{-jA_1y} \tag{2.34}$$

in the free space

$$\tilde{E}_{2z}(w,y) = C_{21}^E(w)e^{jA_2y} + C_{22}^E(w)e^{-jA_2y} \tag{2.35}$$

$$\tilde{H}_{2z}(w,y) = C_{21}^H(w)e^{jA_2y} + C_{22}^H(w)e^{-jA_2y} \tag{2.36}$$

The first boundary condition is the vanishing of the tangential component of the electric field over the ground plane (at $y = 0$):

$$E_{z\ TOT}(x,0) = 0 \ \Rightarrow\ C_{11}^E + C_{12}^E + \tilde{E}_{0z}(w,0) = 0 \ \Rightarrow\ C_{12}^E = -C_{11}^E \tag{2.37}$$

$$E_{x\ TOT}(x,0) = 0 \ \Rightarrow\ \left.\frac{\partial \tilde{H}_{z\ TOT}}{\partial y}\right|_{y=0} = 0 \ \Rightarrow$$

$$\Rightarrow\ jA_1C_{11}^H - jA_1C_{12}^H + \left.\frac{\partial \tilde{H}_{0z}}{\partial y}\right|_{y=0} = 0 \Rightarrow\ C_{12}^H = C_{11}^H \tag{2.38}$$

Then, since the electromagnetic field produced by the microstrip radiates towards infinity and there aren't reflected wave, a radiation condition has to

be imposed on the fields in the free space:

$$E_{z\ TOT}(x, y \to \infty) = 0 \ \Rightarrow \ C_{21}^{E} = 0 \tag{2.39}$$

$$H_{z\ TOT}(x, y \to \infty) = 0 \ \Rightarrow \ C_{21}^{H} = 0 \tag{2.40}$$

Considering the previous condition, the fields become:

inside the dielectric

$$\tilde{E}_{1z}(w, y) = C_1^E \sin(A_1 y) \tag{2.41}$$

$$\tilde{H}_{1z}(w, y) = C_1^H \cos(A_1 y) \tag{2.42}$$

in the free space

$$\tilde{E}_{2z}(w, y) = C_2^E e^{-jA_2 y} \tag{2.43}$$

$$\tilde{H}_{2z}(w, y) = C_2^H e^{-jA_2 y} \tag{2.44}$$

Imposing the continuity of the tangential component of the electric field between the dielectric and the air ($y = d$), the conditions that link the fields in the two regions of space are obtained:

$$E_{z\ TOT}(x, d^+) = E_{z\ TOT}(x, d^-) \ \Rightarrow \ C_1^E sen(A_1 d) = C_2^E e^{-jA_2 d} \tag{2.45}$$

$$E_{x\ TOT}(x, d^+) = E_{x\ TOT}(x, d^-) \ \Rightarrow$$

$$\Rightarrow \ A_1 C_1^H \sin(A_1 d) = [\frac{jk_z w}{\omega\mu} \frac{k_0^2 - k_1^2}{k_2^2 - k_z^2} C_2^E + j \frac{k_1^2 - k_z^2}{k_2^2 - k_z^2} A_2 C_2^H] e^{-jA_2 d} \tag{2.46}$$

Finally, the continuity of the tangential component of the magnetic field between the dielectric and the air has to be imposed. It can be useful to introduce two new functions, namely $J_z(x)$ and $J_x(x)$, that are equal to the longitudinal and the transverse components of the current densities induced on the microstrip if $x \leq a$, zero otherwise. In this way, the last boundary

condition becomes:

$$h_{1x}(x,d) - h_{2x}(x,d) = J_z(x) \tag{2.47}$$

$$h_{2z}(x,d) - h_{1z}(x,d) = J_x(x) \tag{2.48}$$

The same equations, in the spectral domain, become:

$$\tilde{H}_{1x}(w,d) - \tilde{H}_{2x}(w,d) = \tilde{J}_z(w) \tag{2.49}$$

$$\tilde{H}_{2z}(w,d) - \tilde{H}_{1z}(w,d) = \tilde{J}_x(w) \tag{2.50}$$

Of course, the following constrains have to be respected on the current densities, for $|x| > a$:

$$\int_{-\infty}^{+\infty} J_z(w) e^{jwx} dw = 0 \tag{2.51}$$

$$\int_{-\infty}^{+\infty} J_x(w) e^{jwx} dw = 0 \tag{2.52}$$

Using the equation (2.22), the (2.49) becomes:

$$\frac{k_1^2}{k_1^2 - k_z^2} \frac{1}{j\omega\mu} \left[-\frac{\partial \tilde{E}_{1z}}{\partial y} + \frac{jwk_z}{\omega\varepsilon_1} \tilde{H}_{1z} \right] \Bigg|_{y=d} +$$

$$- \frac{k_2^2}{k_2^2 - k_z^2} \frac{1}{j\omega\mu} \left[-\frac{\partial \tilde{E}_{2z}}{\partial y} + \frac{jwk_z}{\omega\varepsilon_0} \tilde{H}_{2z} \right] \Bigg|_{y=d} = \tilde{J}_z(w) \tag{2.53}$$

Substituting the expressions of the fields (2.41), (2.42), (2.43) and (2.44)

in the (2.50) and (2.53), the following equation can be found:

$$\begin{aligned}\tilde{J}_z(w) = &- \frac{k_1^2}{k_1^2 - k_z^2}\frac{C_1^E A_1 \cos(A_1 d)}{j\omega\mu} + \frac{wk_z}{k_1^2 - k_z^2} C_1^H \cos(A_1 d) + \\ &- C_1^E \frac{k_2^2}{k_2^2 - k_z^2}\frac{A_2 \sin(A_1 d)}{\omega\mu} + C_1^H \frac{jA_1}{A_2}\frac{wk_z}{k_1^2 - k_z^2}\sin(A_1 d) + \\ &+ C_1^E \frac{k_z^2 w^2}{\omega\mu}\frac{k_2^2 - k_1^2}{(k_2^2 - k_z^2)(k_1^2 - k_z^2)}\frac{\sin(A_1 d)}{A_2} \qquad (2.54)\\ \tilde{J}_x(w) = &- C_1^H j\frac{A_1}{A_2}\frac{k_2^2 - k_z^2}{k_1^2 - k_z^2}\sin(A_1 d) - C_1^E \frac{k_z w}{\omega\mu}\frac{k_2^2 - k_1^2}{k_1^2 - k_z^2}\frac{\sin(A_1 d)}{A_2} + \\ &- C_1^H \cos(A_1 d) \qquad (2.55)\end{aligned}$$

Considering that:

$$- k_2^2 \frac{k_1^2 - k_z^2}{k_2^2 - k_z^2} A_2^2 + k_z^2 w^2 \frac{k_2^2 - k_1^2}{k_2^2 - k_z^2} = k_z^2(k_2^2 - k_1^2) - k_1^2 A_2 \qquad (2.56)$$

after some manipulation, it's possible to obtain the induced currents as function of the constants C_1^E and C_1^H (that is to say the fields):

$$\begin{aligned}\tilde{J}_z(w) = &\frac{1}{\omega\mu A_2(k_1^2 - k_z^2)}\{C_1^E[jk_1^2 A_1 A_2 \cos(A_1 d) + k_z^2(k_2^2 - k_1^2)\sin(A_1 d) + \\ &- k_1^2 A_2 \sin(A_1 d)] + \frac{C_1^H}{\mu} wk_z[\omega\mu A_2 \cos(A_1 d) + jA_1\omega\mu \sin(A_1 d)]\} \qquad (2.57)\\ \tilde{J}_x(w) = &\frac{1}{\omega\mu A_2(k_1^2 - k_z^2)}\{-C_1^E k_z w(k_2^2 - k_1^2)\sin(A_1 d) + \\ &- C_1^H[j\omega\mu A_1(k_2^2 - k_z^2)\sin(A_1 d) + \omega\mu A_2(k_1^2 - k_z^2)\cos(A_1 d)]\} \qquad (2.58)\end{aligned}$$

That can be better expressed through a matrix:

$$A(w) = jk_1^2 A_1 A_2 \cos(A_1 d) + k_z^2(k_2^2 - k_1^2)\sin(A_1 d) - k_1^2 A_2 \sin(A_1 d) \qquad (2.59)$$

$$B(w) = wk_z\omega\mu[A_2 \cos(A_1 d) + jA_1 \sin(A_1 d)] \qquad (2.60)$$

$$C(w) = -k_z w(k_2^2 - k_1^2)\sin(A_1 d) \qquad (2.61)$$

$$D(w) = -\omega\mu[jA_1(k_2^2 - k_z^2)\sin(A_1 d) + A_2(k_1^2 - k_z^2)\cos(A_1 d)] \qquad (2.62)$$

$$\begin{pmatrix} \tilde{J}_z(w) \\ \tilde{J}_X(w) \end{pmatrix} = \frac{1}{\omega\mu A_2(k_1^2 - k_z^2)} \begin{pmatrix} A(w) & B(w) \\ C(w) & D(w) \end{pmatrix} \begin{pmatrix} C_1^E \\ C_1^H \end{pmatrix} \tag{2.63}$$

As will be shown in the next section, it's more useful to find the expression of the fields as function of the induced currents. For this reason, the matrix of the equation (2.63) has to be inverted, obtaining:

$$\begin{pmatrix} C_1^E \\ C_1^H \end{pmatrix} = \begin{pmatrix} G_{11} & G_{12} \\ G_{21} & G_{22} \end{pmatrix} \begin{pmatrix} \tilde{J}_z \\ \tilde{J}_x \end{pmatrix} \tag{2.64}$$

where

$$G_{11} = \frac{-\omega\mu[-jA_1(k_2^2 - k_z^2)\sin(A_1 d) + A_2(k_1^2 - kz^2)\cos(A_1 d)]}{jA_1A_2k_2^2[\sin^2(A_1 d)(1-\varepsilon_1) - \varepsilon_1] + k_2^2(A_1^2 + \varepsilon_1 A_2^2)\sin(A_1 d)\cos(A_1 d)} \tag{2.65}$$

$$G_{12} = \frac{-wk_z\omega\mu[A_2\cos(A_1 d) + jA_1\sin(A_1 d)]}{jA_1A_2k_2^2[\sin^2(A_1 d)(1-\varepsilon_1) - \varepsilon_1] + k_2^2(A_1^2 + \varepsilon_1 A_2^2)\sin(A_1 d)\cos(A_1 d)} \tag{2.66}$$

$$G_{21} = \frac{k_z w\ (1-\varepsilon_1)\sin(A_1 d)}{jA_1A_2[\sin^2(A_1 d)(1-\varepsilon_1) - \varepsilon_1] + (A_1^2 + \varepsilon_1 A_2^2)\sin(A_1 d)\cos(A_1 d)} \tag{2.67}$$

$$G_{22} = \frac{j\varepsilon_1 A_1 A_2\cos(A_1 d) + [k_z^2(1-\varepsilon_1) - \varepsilon_1 A_2]\sin(A_1 d)}{jA_1A_2[\sin^2(A_1 d)(1-\varepsilon_1) - \varepsilon_1] + (A_1^2 + \varepsilon_1 A_2^2)\sin(A_1 d)\cos(A_1 d)} \tag{2.68}$$

2.4 Solution of the problem

In this section, a perfectly conducting microstrip ($\sigma = \infty$). In the previous section, the electromagnetic field produced by the induced current on the microstrip has been expressed as function of the current itself. To find the unknown current density, the last boundary condition has to be imposed. As the considered microstrip is lossless, the vanishing of the tangential component of the electric field over the microstrip has to be enforced.

$$E_{z\ TOT}(x, y = d) = 0 \quad |x| < a \tag{2.69}$$

$$E_{x\ TOT}(x, y = d) = 0 \quad |x| < a \tag{2.70}$$

In the spectral domain, these equations become:

$$\frac{1}{2\pi}\int_{-\infty}^{+\infty}\tilde{E}_{1z}(w,d)e^{jwx}dw = -\frac{1}{2\pi}\int_{-\infty}^{+\infty}\tilde{E}_{0z}(w,d)e^{jwx}dw \quad |x|<a \tag{2.71}$$

$$\frac{1}{2\pi}\int_{-\infty}^{+\infty}\tilde{E}_{1X}(w,d)e^{jwx}dw = -\frac{1}{2\pi}\int_{-\infty}^{+\infty}\tilde{E}_{0x}(w,d)e^{jwx}dw \quad |x|<a \tag{2.72}$$

By means of the equations (2.41) and (2.20), we obtain:

$$\int_{-\infty}^{+\infty}C_1^E\sin(A_1d)e^{jwx}dw = -\int_{-\infty}^{+\infty}\tilde{E}_{0z}(w,d)e^{jwx}dw \tag{2.73}$$

$$\int_{-\infty}^{+\infty}\left[\frac{-jwk_z}{\omega\mu}C_1^E - A_1C_1^H\right]\sin(A_1d)e^{jwx}dw = \\ = \int_{-\infty}^{+\infty}\left[\frac{-jwk_z}{\omega\mu}\tilde{E}_{0z}(w,d) + \frac{\partial\tilde{H}_{0z}(w,d)}{\partial y}\right]e^{jwx}dw \tag{2.74}$$

Then, the constants C_1^E and C_1^H can be expressed by means of the relation (2.64), so that:

$$\int_{-\infty}^{+\infty}\left[G_{11}\tilde{J}_z(w)+G_{12}\tilde{J}_x(w)\right]\sin(A_1d)e^{jwx}dw = -\int_{-\infty}^{+\infty}\tilde{E}_{0z}(w,d)e^{jwx}dw \tag{2.75}$$

$$\int_{-\infty}^{+\infty}\left[\frac{jwk_z}{\omega\mu}\left[G_{11}\tilde{J}_z(w)+G_{12}\tilde{J}_x(w)\right] - A_1\left[G_{21}\tilde{J}_z(w)+G_{22}\tilde{J}_x(w)\right]\right]\cdot \\ \cdot\sin(A_1d)e^{jwx}dw = \int_{-\infty}^{+\infty}\left[\frac{jwk_z}{\omega\mu}\tilde{E}_{0z}(w,d) - \frac{\partial\tilde{H}_{0z}(w,d)}{\partial y}\right]e^{jwx}dw \tag{2.76}$$

These equations and the (2.51) and (2.52) are a dual system of integral equations, whose solutions allow to evaluate the unknown induced current

densities and then the electromagnetic field:

$$\begin{cases} \qquad\qquad for\,|x| < a \\ \int_{-\infty}^{+\infty} \left[G_{11}\tilde{J}_z(w) + G_{12}\tilde{J}_x(w)\right] \sin(A_1 d) e^{jwx} dw = -\int_{-\infty}^{+\infty} \tilde{E}_{0z}(w,d) e^{jwx} dw \\ \int_{-\infty}^{+\infty} \left[\frac{jwk_z}{\omega\mu}\left[G_{11}\tilde{J}_z(w) + G_{12}\tilde{J}_x(w)\right] - A_1\left[G_{21}\tilde{J}_z(w) + G_{22}\tilde{J}_x(w)\right]\right] \cdot \\ \qquad \cdot \sin(A_1 d) e^{jwx} dw = \int_{-\infty}^{+\infty} \left[\frac{jwk_z}{\omega\mu}\tilde{E}_{0z}(w,d) - \frac{\partial \tilde{H}_{0z}(w,d)}{\partial y}\right] e^{jwx} dw \\ \\ \qquad\qquad for\,|x| > a \\ \int_{-\infty}^{+\infty} J_z(w) e^{jwx} dw = 0 \\ \int_{-\infty}^{+\infty} J_x(w) e^{jwx} dw = 0 \end{cases} \tag{2.77}$$

The system can be efficiently solved representing the current densities by means of a Neumann series, namely a series of Bessel functions of variable index. In general, the Neumann series can be expressed as follows:

$$\sum_{n=0}^{\infty} F_n \frac{J_{n+s}(\alpha w)}{(\alpha w)^s} \tag{2.78}$$

The investigation of the most general series is due to Gegenbauer and the representability in Neumann series has been analysed by Watson in its famous treatise on the Bessel functions [11]: the representability condition is translated in a complicated integral equation, so the method results very hard to use. The problem has been recently reconsidered by Eswaran, who has analyzed the problem more accurately and he has an easy way to use these series [15]. In particular, it has been demonstrated that a function whose Fourier transform has compact support, that is to say null outside of an ended domain, can be expanded in Neumann series. Now, the last two equations of the dual system just express this property. For this reason, the current densities $J_z(w)$ and

$J_x(w)$ are expanded as follows:

$$\tilde{J}_z(w) = A\sum_{n=0}^{\infty} F_{zn}\frac{J_{n+s}(wa)}{(wa)^s} \tag{2.79}$$

$$\tilde{J}_x(w) = A\sum_{n=0}^{\infty} F_{xn}\frac{J_{n+p}(wa)}{(wa)^p} \tag{2.80}$$

The quantities F_{zn} and F_{xn} are dimensionless unknown expansion coefficients, while A is only a normalizing constant. To understand how this expansion can be useful, a relevant integral on the Bessel functions has to be invoked:

$$\int_{-\infty}^{\infty} \frac{J_{n+p}(wa)}{(wa)^s} e^{jwx} dw = \begin{cases} \frac{2^s j^n n!\Gamma(s)}{a\Gamma(2s+n)}\left[1-\left(\frac{x}{a}\right)^2\right]^{s-\frac{1}{2}} C_n^s\left(\frac{x}{a}\right) & x < a \\ 0 & x > a \end{cases} \tag{2.81}$$

$$\int_{-a}^{a} \left[1-\left(\frac{x}{a}\right)^2\right]^{s-\frac{1}{2}} C_n^s\left(\frac{x}{a}\right) e^{-jwx} dx = \frac{a\pi 2^{1-s}\Gamma(2s+n)}{j^n n!\Gamma(s)}\frac{J_{n+s}(wa)}{(wa)^s} \tag{2.82}$$

The functions $C_m^s(x)$ are Gegenbauer polynomials (see Appendix 1).

For $x < a$, the equation (2.81) gives a way to analytically transform the Neumann series, so that the expression of the induced currents in the spatial domain can be easily computed and used for further analyses. Then, a proper choice of the parameter s in the series allows to factorise the right edge behaviour of the current, so only a continuos function has to be represented (by means of Gegenbauer polynomials), producing a fast convergence of the method. On the other hand, for $x > a$ the (2.81) states that the last two equations of the (2.77) are already satisfied if the current densities are expanded in Neumann series.

Thus, the equations (2.79) and (2.80) are substituted in the (2.77):

$$\begin{cases} A\sum_{n=0}^{+\infty}\left\{F_{zn}\int_{-\infty}^{+\infty}\frac{J_{n+s}(wa)}{(wa)^s}G_{11}\sin(A_1d)e^{jwx}dw+\right. \\ \quad \left.+F_{xn}\int_{-\infty}^{+\infty}\frac{J_{n+p}(wa)}{(wa)^p}\cdot G_{12}\sin(A_1d)e^{jwx}dw\right\}=-\int_{-\infty}^{+\infty}\tilde{E}_{0z}(w,d)e^{jwx}dw \\ A\sum_{n=0}^{+\infty}\left\{F_{zn}\int_{-\infty}^{+\infty}\frac{J_{n+s}(wa)}{(wa)^s}\left(\frac{jwk_z}{\omega\mu}G_{11}-A_1G_{21}\right)\sin(A_1d)e^{jwx}dw+\right. \\ \quad \left.+F_{xn}\int_{-\infty}^{+\infty}\frac{J_{n+p}(wa)}{(wa)^p}\left(\frac{jwk_z}{\omega\mu}G_{12}-A_1G_{22}\right)\sin(A_1d)e^{jwx}dw=\right. \\ \quad =\int_{-\infty}^{+\infty}\left[\frac{jwk_z}{\omega\mu}\tilde{E}_{0z}(w,d)-\frac{\partial\tilde{H}_{0z}(w,d)}{\partial y}\right]e^{jwx}dw \end{cases} \tag{2.83}$$

These equations have to be verified $\forall x : |x| \leq a$. There are different solutions to impose this condition. One can be projecting the equations in the same functional space used to expand the current densities. That can be done multiplying the equations (2.83) by the quantity:

$$\frac{1}{2\pi a}\left[1-\left(\frac{x}{a}\right)^2\right]^{r-\frac{1}{2}}C_m^r\left(\frac{x}{a}\right) \tag{2.84}$$

Then, integrating the resulting equations in dx between $-a$ and a, using the relevant integral (2.82), we finally obtain:

$$\begin{cases} A\sum_{n=0}^{+\infty}\left\{F_{zn}\int_{-\infty}^{+\infty}\frac{J_{n+s}(wa)}{(wa)^s}\frac{J_{m+r}(wa)}{(wa)^r}G_{11}\sin(A_1d)dw+\right. \\ \quad +F_{xn}\int_{-\infty}^{+\infty}\frac{J_{n+p}(wa)}{(wa)^p}\frac{J_{m+r}(wa)}{(wa)^r}G_{12}\sin(A_1d)dw= \\ \quad =-\int_{-\infty}^{+\infty}\tilde{E}_{0z}(w,d)\frac{J_{m+r}(wa)}{(wa)^r}dw \\ A\sum_{n=0}^{+\infty}\left\{F_{zn}\int_{-\infty}^{+\infty}\frac{J_{n+s}(wa)}{(wa)^s}\frac{J_{m+t}(wa)}{(wa)^t}\left(\frac{jwk_z}{\omega\mu}G_{11}-A_1G_{21}\right)\sin(A_1d)dw+\right. \\ \quad \left.+F_{xn}\int_{-\infty}^{+\infty}\frac{J_{n+p}(wa)}{(wa)^p}\frac{J_{m+t}(wa)}{(wa)^t}\left(\frac{jwk_z}{\omega\mu}G_{12}-A_1G_{22}\right)\sin(A_1d)dw\right\}= \\ \quad =\int_{-\infty}^{+\infty}\left[\frac{jwk_z}{\omega\mu}\tilde{E}_{0z}(w,d)-\frac{\partial\tilde{H}_{0z}(w,d)}{\partial y}\right]\frac{J_{m+t}(wa)}{(wa)^t}dw \end{cases} \tag{2.85}$$

After that, the system of integral equations has been reduced to an algebraic system, whose easy solution allows to evaluate the coefficients F_{zn} and F_{xn}.

At this point, a proper choice has to be done on the parameters s and p. A first constrain is due to the convergence of the integrals. This means that the following condition has to be respected:

$$s > -\frac{1}{2} \qquad and \qquad p > \frac{1}{2} \tag{2.86}$$

A further constrain on such parameters in given imposing the right edge behaviour of the current densities. From the integral (2.82), it can be seen that the edge behaviour of the expansion (2.79) is given by the term:

$$\left[1 - \left(\frac{x}{a}\right)^2\right]^{s-\frac{1}{2}} \tag{2.87}$$

As the microstrip is perfectly conducting and of infinitesimal thickness, the longitudinal component of the current, $J_z(x)$, has to show, for $x \to a$, a behaviour like $1 \Big/ \sqrt{1-(x/a)^2}$. For this reason, the right choice is $\underline{s = 0}$.

For the same reason, considering that the transverse component of the current density, $J_x(x)$, has to show, for $x \to a$, a behaviour like $\sqrt{1-(x/a)^2}$, the proper choice is $\underline{p = 1}$.

With these choices, the transform of the current densities, performed by means of the integral (2.82), can be particularised of follows:

$$\tilde{J}_z(x) = A\frac{1}{a\pi}\left[1 - \left(\frac{x}{a}\right)^2\right]^{-\frac{1}{2}} \sum_{n=0}^{\infty} (-j)^n F_{zn} T_n\left(\frac{x}{a}\right) \tag{2.88}$$

$$\tilde{J}_x(x) = A\frac{1}{a\pi}\left[1 - \left(\frac{x}{a}\right)^2\right]^{\frac{1}{2}} \sum_{n=0}^{\infty} \frac{(-j)^n}{n} F_{xn} U_n\left(\frac{x}{a}\right) \tag{2.89}$$

Note that the Gegenbauer polynomials turn into Chebyshev polynomials of first and second kind, as described in Appendix 1.

Finally, the value of the parameters r and t, introduced in the system 2.85 by the projection, has to be chosen. There isn't a physical reason in this

choice, but only a computational convenience: it has been demonstrated that the conditions $r = s$ and $p = t$ assure that the matrix of the algebraic system exhibits a diagonal dominance, that is a desirable for the inversion.

2.5 Evaluation of the integrals

After the use of the Neumann series, the problem has been reduced to the solution of an algebraic system. Some considerations can be done on the matrix of this system, and in particular on the integrals that are the elements of this matrix. The following elements can be defined:

$$I_{1\,n,m} = F_{zn} \int_{-\infty}^{+\infty} \frac{J_{n+s}(wa)}{(wa)^s} \frac{J_{m+r}(wa)}{(wa)^r} G_{11} sen(A_1 d) dw \tag{2.90}$$

$$I_{2\,n,m} = F_{xn} \int_{-\infty}^{+\infty} \frac{J_{n+p}(wa)}{(wa)^p} \frac{J_{m+r}(wa)}{(wa)^r} G_{12} sen(A_1 d) dw \tag{2.91}$$

$$I_{3\,n,m} = F_{zn} \int_{-\infty}^{+\infty} \frac{J_{n+s}(wa)}{(wa)^s} \frac{J_{m+t}(wa)}{(wa)^t} \left(-G_{11} \frac{wk_z}{k^2 - k_z^2} + \right.$$
$$\left. -G_{21} \frac{k^2}{k^2 - k_z^2} \frac{A_1}{j\omega\varepsilon} \right) sen(A_1 d) dw \tag{2.92}$$

$$I_{4\,n,m} = F_{xn} \int_{-\infty}^{+\infty} \frac{J_{n+p}(wa)}{(wa)^p} \frac{J_{m+t}(wa)}{(wa)^t} \left(-G_{12} \frac{wk_z}{k^2 - k_z^2} + \right.$$
$$\left. -G_{22} \frac{k^2}{k^2 - k_z^2} \frac{A_1}{j\omega\varepsilon} \right) sen(A_1 d) dw \tag{2.93}$$

Then, the matrix of the system can be written as follows:

$$\begin{bmatrix} I_1 & I_2 \\ I_3 & I_4 \end{bmatrix} \tag{2.94}$$

To fill efficiently the matrix, some consideration can be done. First of all,

each of the sub-matrix I_1, I_2, I_3 and I_4 exhibits a symmetry with respect to the principal diagonal, that is to say:

$$I_{i\,m,n} = I_{i\,n,m} \tag{2.95}$$

Then, considered that the Bessel functions of integer order are even or odd as the order of the function itself. So considering the parity of the functions multiplied for the Bessel ones, some integrals vanish. In particular, all the integrals contained in I_1 and I_4 are zero if $n + m$ is odd while the integrals contained in I_2 and I_3 are zero if $n + m$ is even.

All these considerations on the integrals reduce the number of integrals to evaluate.

Other considerations must be done on the computation of the integrals. The Bessel functions are asymptotically oscillating and slowly convergent, so the time required to numerically evaluate the integrals could be relevant. For this reason, it could be useful to study the asymptotic behaviour of kernels of the integrals. For example, let us consider the sub-matrix I_1, that is to say the integral:

$$\int_{-\infty}^{+\infty} \frac{J_{n+s}(wa)}{(wa)^s} \frac{J_{m+r}(wa)}{(wa)^r} G_{11} sen(A_1 d) dw \tag{2.96}$$

It's possible to expand the function G_{11} in inverse powers of w, something like that:

$$G(w) = c_0 + \frac{c_1}{w} + \frac{c_2}{w^2} + \dots \tag{2.97}$$

Of course only a finite number of expansion terms can be considered: for example two expansions terms are considered. In that case, the integral (2.96) can be written as follows:

$$\begin{aligned} &\int_{-\infty}^{+\infty} \frac{J_{n+s}(wa)}{(wa)^s} \frac{J_{m+r}(wa)}{(wa)^r} \left[G(w) - c_0 - \frac{c_1}{w} \right] dw + \\ &+ \int_{-\infty}^{+\infty} \left[c_0 + \frac{c_1}{w} \right] \frac{J_{n+s}(wa)}{(wa)^s} \frac{J_{m+r}(wa)}{(wa)^r} dw \end{aligned} \tag{2.98}$$

Of course the first integral has a faster convergence than the (2.96). This trick is useful if the second integral can be evaluated analytically. That is possible, through the relevant integral [22]:

$$\int_0^{+\infty} J_\mu(\alpha t)J_\nu(\alpha t)t^{-\lambda}dt = \frac{\alpha^{\lambda-1}}{2^\lambda}\frac{\Gamma(\lambda)\Gamma\left(\frac{\mu+\nu-\lambda+1}{2}\right)}{\Gamma\left(\frac{\mu+\nu+\lambda+1}{2}\right)\Gamma\left(\frac{\mu-\nu+\lambda+1}{2}\right)\Gamma\left(\frac{-\mu+\nu+\lambda+1}{2}\right)} \quad (2.99)$$

Of course, as many terms of the expansion (2.97) are used, as faster the integral in evaluated numerically. Anyway, the choice of the number of terms to be subtract to the kernel is a compromise asymptotical between the rapidity and the simplicity to analytically solve the residual integral.

A critical situation happens when $\mu = \nu = 0$ and $\lambda = 1$, because the integral diverges, due to the singularity in the origin, that is to say:

$$\int_{-\infty}^{+\infty} \frac{1}{w}J_0(w\alpha)J_0(w\alpha)dw = \infty \quad (2.100)$$

The problem can be easily revolved using another function that doesn't exhibit the singularity in the origin but the same behaviour of the function $1/w$. A possible choice can be:

$$\frac{w}{w^2+q^2} \quad (2.101)$$

That solution is suggested by a relevant integral:

$$\int_{-\infty}^{+\infty} \frac{w}{w^2+q}J_0(w\alpha)J_0(w\alpha)dw = I_0(\alpha q)K_0(\alpha q) \quad (2.102)$$

The parameter q has to be chosen properly.

2.6 Numerical results

In this section, some numerical results are presented, considering as forcing field a wire of current of a plane wave TM and TE polarized. These are the

values used for all the simulations (if not specified differently): $a = 1\,mm$ (microstrip half width), $d = 1\,mm$ (dielectric thickness), $\varepsilon_r = 9.2$ (dielectric relative permittivity), $f = 1\,GHz$ (frequency).

The system (2.85) has been written in the most generic form. Depending on the forcing field used, the terms of the system have to be particularized and some of them may vanish. For example, if the source is a wire of current or a plane wave TM polarized (described in appendix B), only the current density $J_z(x)$ is present.

First of all, a wire of current is assumed as forcing field. The matrix of the system is plotted to evidence the diagonal dominance (figure 2.2).

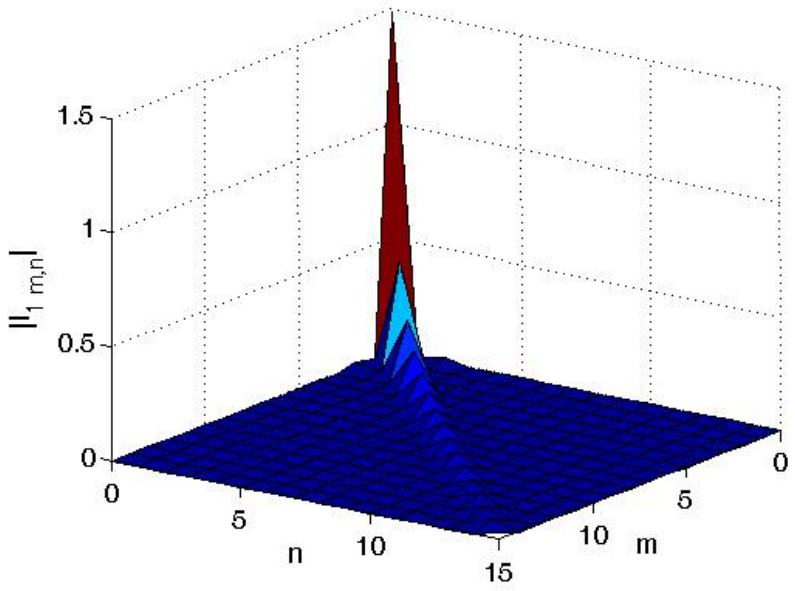

Figure 2.2: Lossless microstrip: Amplitude of the matrix of the system

Then, placing the wire in $\alpha = 0.5mm$ and at different heights, the expansion coefficients and the induced current densities are shown (figures 2.3 and 2.4). Few coefficients are needed to have a good accuracy. The results are also compared with the ones produced by a FEM solver, *Maxwll 2D* by Ansoft, exhibiting a good agreement. Of course the FEM solver becomes inadequate to evaluate the current density at the edges of the microstrip, as a numerical method can't reproduce accurately a divergent variable.

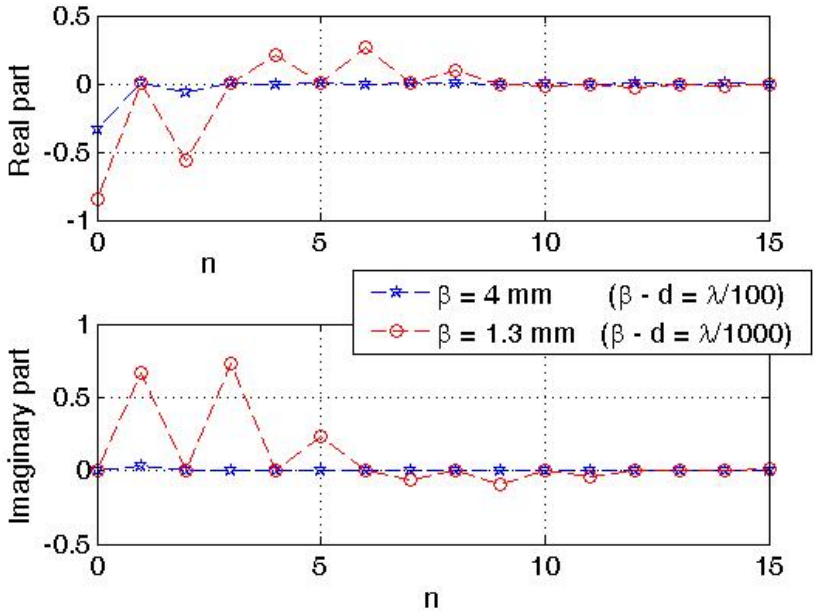

Figure 2.3: Lossless microstrip: Expansion coefficients of current densities induced by a wire

Also a plane wave TM polarized is considered as forcing field, in particular when the propagation vector is in the y, z plane ($k_z \neq 0$). In the following figures 2.5 and 2.6, the expansion coefficients and the induced current densities are shown for different incidence angles.

Finally, the same simulations are performed with a plane wave TE polarized (figures 2.7 and 2.8), always when the propagation vector is in the y, z plane ($k_z \neq 0$).

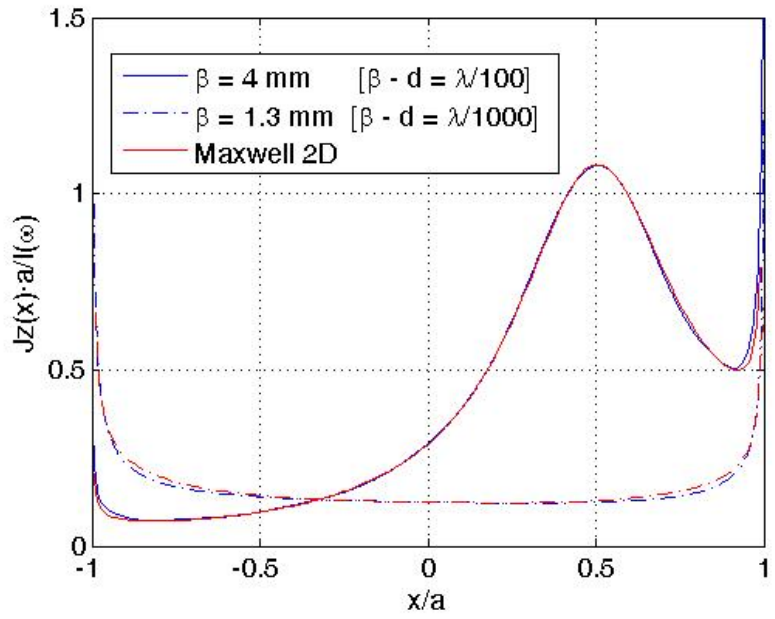

Figure 2.4: Lossless microstrip: Current densities induced by a wire, for different distances, and comparison with a FEM solver

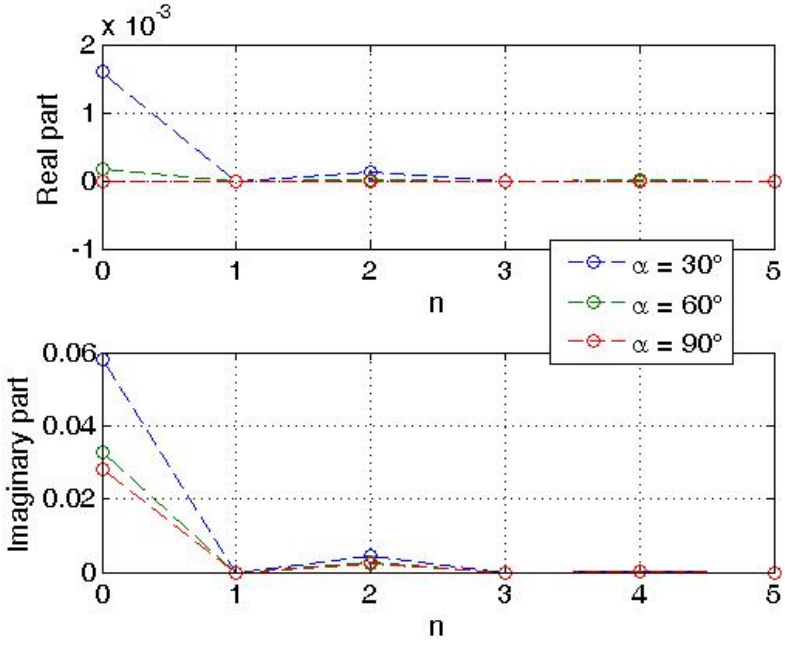

Figure 2.5: Lossless microstrip: Expansion coefficients of current densities induced by a plane wave TM polarized

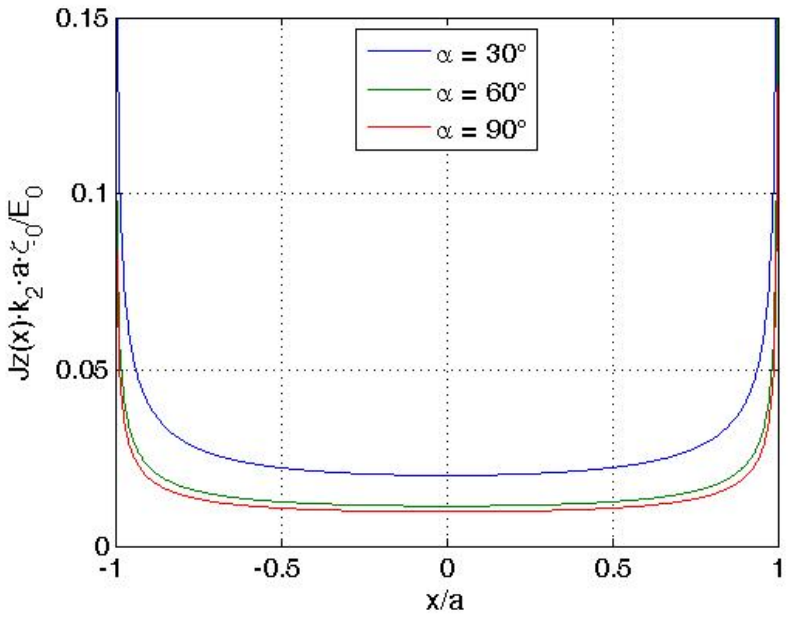

Figure 2.6: Lossless microstrip: Current densities induced by a plane wave TM polarized, for different incidence angles

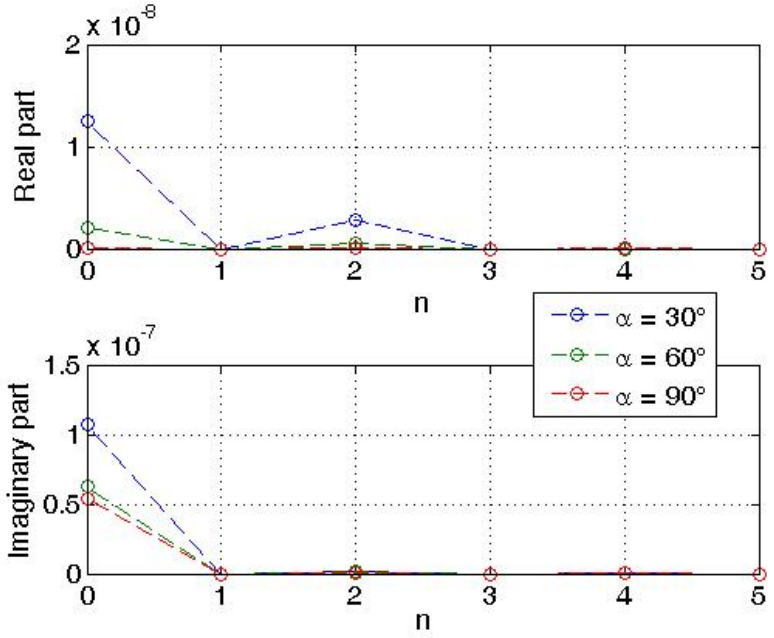

Figure 2.7: Lossless microstrip: Expansion coefficients of current densities induced by a plane wave TE polarized

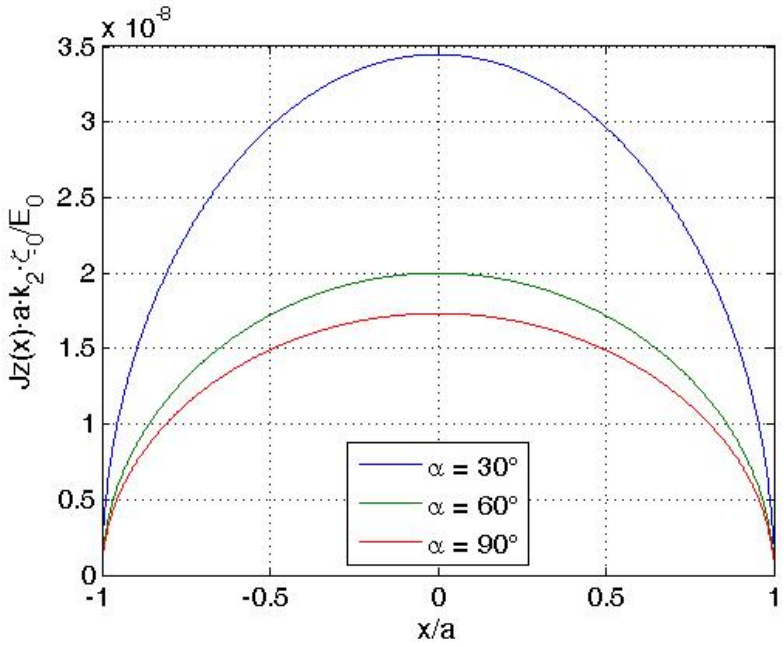

Figure 2.8: Lossless microstrip: Current densities induced by a plane wave TE polarized, for different incidence angles

Chapter 3

Microstrip of finite conductivity

In this chapter, the method previously presented is adopted to analyze a microstrip of finite conductivity. Then, the method is extended to the case of two coupled microstrips, with a minimum increase of computational effort.

3.1 Formulation and solution of the problem

As the microstrip has an infinitesimal thickness, the finite conductivity is introduced through the Leontovich surface impedance ζ, defined as:

$$\zeta = \sqrt{\mu_0 / \left(\varepsilon_0 - j\sigma/\omega\right)} \tag{3.1}$$

where σ is the conductivity of the microstrip. The validity of this model has been already discussed in chapter 1.

Following this approach, the formulation presented in section 2.3 can be repeated identically. The difference is the boundary condition to impose on the microstrip, that now is:

$$\vec{E}_{TOT}(x, y = d) = \zeta \vec{H}_{TOT}(x, y = d) \times \hat{n} \qquad |x| < a \tag{3.2}$$

That means:

$$E_{z\,TOT}(x, y = d) = \zeta H_{x\,TOT}(x, y = d) \tag{3.3}$$

$$E_{x\,TOT}(x, y = d) = \zeta H_{z\,TOT}(x, y = d) \tag{3.4}$$

In the spectral domain, these equations become:

$$\frac{1}{2\pi}\int_{-\infty}^{+\infty}\left[\tilde{E}_{1z}(w,d)-\zeta\tilde{H}_{1x}(w,d)\right]e^{jwx}dw = \\ = -\frac{1}{2\pi}\int_{-\infty}^{+\infty}\left[\tilde{E}_{0z}(w,d)-\zeta\tilde{H}_{0x}(w,d)\right]e^{jwx}dw \tag{3.5}$$

$$\frac{1}{2\pi}\int_{-\infty}^{+\infty}\left[\tilde{E}_{1x}(w,d)+\zeta\tilde{H}_{1z}(w,d)\right]e^{jwx}dw = \\ = -\frac{1}{2\pi}\int_{-\infty}^{+\infty}\left[\tilde{E}_{0x}(w,d)+\zeta\tilde{H}_{0z}(w,d)\right]e^{jwx}dw \tag{3.6}$$

Using the equations (2.41), (2.42), (2.20) and (2.22), after some operations:

$$\int_{-\infty}^{+\infty}\left[C_1^E\sin(A_1d)-\zeta\frac{k_2^2}{k_2^2-k_z^2}\frac{1}{j\omega\mu}\left(-A_1C_1^E-\frac{jwk_z}{\omega\varepsilon}C_1^H\right)\cos(A_1d)\right]e^{jwx}dw = \\ = -\int_{-\infty}^{+\infty}\left[\tilde{E}_{0z}(w,d)+\zeta\frac{k_2^2}{k_2^2-k_z^2}\frac{1}{j\omega\mu}\left(\frac{\partial\tilde{E}_{0z}}{\partial y}(w,d)+\frac{jwk_z}{\omega\varepsilon}\tilde{H}_{0z}(w,d)\right)\right]e^{jwx}dw \tag{3.7}$$

$$\int_{-\infty}^{+\infty}\left[\frac{k_2^2}{k_2^2-k_z^2}\frac{1}{j\omega\varepsilon}\left(\frac{-jwk_z}{\omega\mu}C_1^E-A_1C_1^H\right)\sin(A_1d)+\zeta C_1^H\cos(A_1d)\right]e^{jwx}dw = \\ = -\int_{-\infty}^{+\infty}\left[\frac{k_2^2}{k_2^2-k_z^2}\frac{1}{j\omega\varepsilon}\left(\frac{-jwk_z}{\omega\mu}\tilde{E}_{0z}(w,d)+\frac{\partial\tilde{H}_{0z}(w,d)}{\partial y}\right)+\zeta\tilde{H}_{0z}(w,d)\right]e^{jwx}dw \tag{3.8}$$

Then, the relation (2.63) between the constants C_1^E, C_1^H and the current densities has to be used. To simplify the notation, it's convenient to make

some positions:

$$M_{11} = G_{11}\sin(A_1 d) + \left(G_{11}\frac{k_2^2}{k_2^2 - k_z^2}\zeta\frac{A_1}{j\omega\mu} + G_{21}\frac{\zeta w k_z}{k_2^2 - k_z^2}\right)\cos(A_1 d) \tag{3.9}$$

$$M_{12} = G_{12}\sin(A_1 d) + \left(G_{12}\frac{k_2^2}{k_2^2 - k_z^2}\frac{\zeta A_1}{j\omega\mu} + G_{22}\frac{\zeta w k_z}{k_2^2 - k_z^2}\right)\cos(A_1 d) \tag{3.10}$$

$$M_{21} = \zeta G_{21}\cos(A_1 d) - \left(G_{11}\frac{w k_z}{k_2^2 - k_z^2} + G_{21}\frac{k_2^2}{k_2^2 - k_z^2}\frac{A_1}{j\omega\varepsilon}\right)\sin(A_1 d) \tag{3.11}$$

$$M_{22} = \zeta G_{22}\cos(A_1 d) - \left(G_{12}\frac{w k_z}{k_2^2 - k_z^2} + G_{22}\frac{k_2^2}{k_2^2 - k_z^2}\frac{A_1}{j\omega\varepsilon}\right)\sin(A_1 d) \tag{3.12}$$

$$N_1 = \tilde{E}_{0z}(w,d) + \zeta\frac{k_2^2}{k_2^2 - k_z^2}\frac{1}{j\omega\mu}\left(\frac{\partial\tilde{E}_{0z}}{\partial y}(w,d) + \frac{j w k_z}{\omega\varepsilon}\tilde{H}_{0z}(w,d)\right) \tag{3.13}$$

$$N_2 = \frac{k_2^2}{k_2^2 - k_z^2}\frac{1}{j\omega\varepsilon}\left(\frac{-j w k_z}{\omega\mu}\tilde{E}_{0z}(w,d) + \frac{\partial\tilde{H}_{0z}}{\partial y}(w,d)\right) + \zeta\tilde{H}_{0z}(w,d) \tag{3.14}$$

After these positions, using the (2.63) in the (3.7) and (3.8), the following equations are finally obtained:

$$\int_{-\infty}^{+\infty}\left(\tilde{J}_z(w)M_{11} + \tilde{J}_x(w)M_{12}\right)e^{jwx}dw = -\int_{-\infty}^{+\infty}N_1\,e^{jwx}dw \tag{3.15}$$

$$\int_{-\infty}^{+\infty}\left(\tilde{J}_z(w)M_{21} + \tilde{J}_x(w)M_{22}\right)e^{jwx}dw = -\int_{-\infty}^{+\infty}N_2\,e^{jwx}dw \tag{3.16}$$

These equations are valid for $|x| < a$. Two others have to be added to the previous, valid for $|x| > a$, that are:

$$\int_{-\infty}^{+\infty}\tilde{J}_z(w)e^{jwx}dw = 0 \tag{3.17}$$

$$\int_{-\infty}^{+\infty}\tilde{J}_x(w)e^{jwx}dw = 0 \tag{3.18}$$

These four equations are dual system of integral equation. Again, it's possible to use the Neumann series to solve this system. By means of the expansions

(2.79) and (2.80), the equations (3.17) and (3.18) are already satisfied, while the (3.15) and (3.16) become:

$$A\sum_{n=0}^{+\infty} F_{zn} \int_{-\infty}^{+\infty} \frac{J_{n+s}(wa)}{(wa)^s} M_{11} e^{jwx} dw + F_{xn} \int_{-\infty}^{+\infty} \frac{J_{n+p}(wa)}{(wa)^p} M_{12} e^{jwx} dw =$$

$$= - \int_{-\infty}^{+\infty} N_1 \, e^{jwx} dw \tag{3.19}$$

$$A\sum_{n=0}^{+\infty} F_{zn} \int_{-\infty}^{+\infty} \frac{J_{n+s}(wa)}{(wa)^s} M_{21} e^{jwx} dw + F_{xn} \int_{-\infty}^{+\infty} \frac{J_{n+p}(wa)}{(wa)^p} M_{22} e^{jwx} dw =$$

$$= - \int_{-\infty}^{+\infty} N_2 \, e^{jwx} dw \tag{3.20}$$

The equations are finally projected, as described in section 2.4, to finally obtain a system of algebraic equations:

$$A\sum_{n=0}^{+\infty} F_{zn} \int_{-\infty}^{+\infty} \frac{J_{n+s}(wa)}{(wa)^s} \frac{J_{m+r}(wa)}{(wa)^r} M_{11} dw + F_{xn} \int_{-\infty}^{+\infty} \frac{J_{n+p}(wa)}{(wa)^p} \frac{J_{m+r}(wa)}{(wa)^r} M_{12} dw =$$

$$= - \int_{-\infty}^{+\infty} \frac{J_{m+r}(wa)}{(wa)^r} N_1 dw \tag{3.21}$$

$$A\sum_{n=0}^{+\infty} F_{zn} \int_{-\infty}^{+\infty} \frac{J_{n+s}(wa)}{(wa)^s} \frac{J_{m+t}(wa)}{(wa)^t} M_{21} dw + F_{xn} \int_{-\infty}^{+\infty} \frac{J_{n+p}(wa)}{(wa)^p} \frac{J_{m+t}(wa)}{(wa)^t} M_{22} dw =$$

$$= - \int_{-\infty}^{+\infty} \frac{J_{m+t}(wa)}{(wa)^t} N_2 dw \tag{3.22}$$

Also in this case, some considerations have to be done on the parameters s and p. The choice adopted in the section 2.4 is incorrect, as the edge behaviour of the current densities is changed according to the new boundary condition on the microstrip. At the moment, there isn't an adequate theory to justify the correct edge behaviour of the current densities. So it's not possible to

find the correct value of these parameters by physical considerations. Anyway, a correct choice of the parameters s and p allows to minimize the expansion coefficients, because if the edge behaviour is already factorized, only a continuous function has to be represented. For this reason, it's possible to perform different simulations, finding that the values able to minimize the expansion coefficients are s=1/2 and p=1/2.

With these choices, the transform of the current densities assumes the following expressions:

$$\tilde{J}_z(x) = A\frac{1}{a\sqrt{2\pi}}\sum_{n=0}^{\infty}(-j)^n F_{zn} P_n\left(\frac{x}{a}\right) \tag{3.23}$$

$$\tilde{J}_x(x) = A\frac{1}{a\sqrt{2\pi}}\sum_{n=0}^{\infty}(-j)^n F_{xn} P_n\left(\frac{x}{a}\right) \tag{3.24}$$

In this case the Gegenbauer polynomials turn into Legendre polynomials, as described in Appendix 1. It's possible to make consideration on the matrix of the system and on the integrals exactly as in section 2.5.

3.2 Coupled microstrips

Before analysing some numerical results, it's interesting to show how the presented method can be easily extended to study two coupled microstrips.

To simplify the study, the two microstrips are supposed to have the same width (a). The distance of the centres of the microstrip from the origin is b.

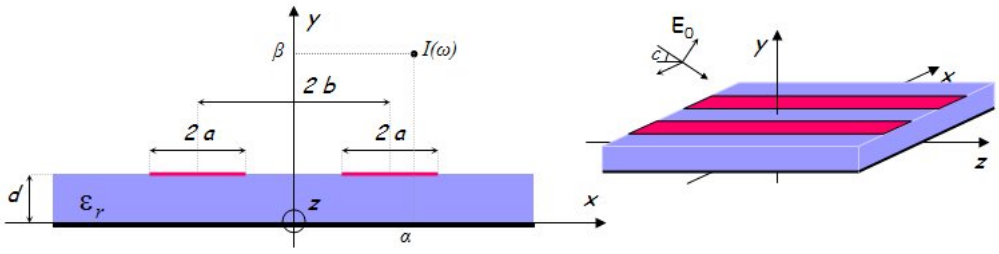

Figure 3.1: Two coupled microstrips

It's simple to observe that the formulation presented in section 3.1 can

be repeated with some small corrections. If the current densities on the left and right microstrip respectively are called $\vec{J}'(x)$ and $\vec{J}''(x)$, the dual system of integral equations, composed by the (3.15), (3.16), (3.17), (3.18), can be written as follows:

$$\begin{cases} \int_{-\infty}^{+\infty} \left\{ [\tilde{J}'_z(w) + \tilde{J}''_z(w)]M_{11} + [\tilde{J}'_x(w) + \tilde{J}''_z(w)]M_{12} \right\} e^{jwx} dw = \\ \qquad = -\int_{-\infty}^{+\infty} N_1\, e^{jwx} dw \qquad for\ |x-b| < a\ and\ for\ |x+b| < a \qquad (3.25) \\ \int_{-\infty}^{+\infty} \left\{ [\tilde{J}'_z(w) + \tilde{J}''_z(w)]M_{21} + [\tilde{J}'_x(w) + \tilde{J}''_x(w)]M_{22} \right\} e^{jwx} dw = \\ \qquad = -\int_{-\infty}^{+\infty} N_2\, e^{jwx} dw \qquad for\ |x-b| < a\ and\ for\ |x+b| < a \qquad (3.26) \\ \int_{-\infty}^{+\infty} \tilde{J}'_z(w) e^{jwx} dw = 0, \quad \int_{-\infty}^{+\infty} \tilde{J}'_x(w) e^{jwx} dw = 0 \qquad for\ |x+b| < a \qquad (3.27) \\ \int_{-\infty}^{+\infty} \tilde{J}''_z(w) e^{jwx} dw = 0, \quad \int_{-\infty}^{+\infty} \tilde{J}''_x(w) e^{jwx} dw = 0 \qquad for\ |x-b| < a \qquad (3.28) \end{cases}$$

The last four equations of the system state that the current densities have to vanish outside the microstrips. That means that the Neumann series has to be adapted to the new positions of the microstrip, as the previous expansions (2.79) and (2.80) are null for $|x| > a$. This translation of the domains can be easily made by multiplying the previous Neumann series for some opportune exponentials:

$$\tilde{J}'_z(w) = A \sum_{n=0}^{\infty} F'_{zn} e^{+jbw} \frac{J_{n+s}(wa)}{(wa)^s},\ \tilde{J}''_z(w) = A \sum_{n=0}^{\infty} F''_{zn} e^{-jbw} \frac{J_{n+s}(wa)}{(wa)^s} \qquad (3.29)$$

$$\tilde{J}'_x(w) = A \sum_{n=0}^{\infty} F'_{xn} e^{+jbw} \frac{J_{n+p}(wa)}{(wa)^p},\ \tilde{J}''_x(w) = A \sum_{n=0}^{\infty} F''_{xn} e^{-jbw} \frac{J_{n+p}(wa)}{(wa)^p} \qquad (3.30)$$

This small change allows to satisfy the equations (3.27) and (3.28), as the transform of the Neumann series now is:

$$\int_{-\infty}^{+\infty} \frac{J_{n+s}(aw)}{(aw)^s} e^{jw(x\mp b)} dw = \begin{cases} \frac{2^s j^n n! \Gamma(s)}{a\Gamma(2s+n)} \left[1 - \left(\frac{x\pm b}{a}\right)^2\right]^{s-\frac{1}{2}} C_n^s\left(\frac{x\pm b}{a}\right) & |x \pm b| < a \\ 0 & |x \pm b| > a \end{cases} \tag{3.31}$$

After using the expansions of the current densities (3.29) and (3.30) in the remaining equations of the dual system (3.25) and (3.26), these equations have to be projected in the two functional spaces used to expand the current densities, that is to say multiplying the equations separately by the quantities:

$$\frac{1}{2\pi a}\left[1 - \left(\frac{x \pm b}{a}\right)^2\right]^{r-\frac{1}{2}} C_m^r\left(\frac{x \pm b}{a}\right) \tag{3.32}$$

and integrating the resulting equations in dx between $-a$ and a.

From these operations, four expressions that compose a system of algebraic equations are obtained. The first two expressions are found from the equation (3.25), choosing the signs + and − in the (3.32).

$$\begin{aligned} &A\sum_{n=0}^{+\infty} J'_{zn} \int_{-\infty}^{+\infty} \frac{J_{n+s}(wa)}{(wa)^s}\frac{J_{m+r}(wa)}{(wa)^r} M_{11} dw + J''_{zn} \int_{-\infty}^{+\infty} \frac{J_{n+s}(wa)}{(wa)^s}\frac{J_{m+r}(wa)}{(wa)^r} M_{11} e^{j2bw} dw + \\ &+ J'_{xn} \int_{-\infty}^{+\infty} \frac{J_{n+p}(wa)}{(wa)^p}\frac{J_{m+r}(wa)}{(wa)^r} M_{12} dw + J''_{xn} \int_{-\infty}^{+\infty} \frac{J_{n+p}(wa)}{(wa)^p}\frac{J_{m+r}(wa)}{(wa)^r} M_{12} e^{j2bw} dw = \\ &= -\int_{-\infty}^{+\infty} \frac{J_{m+r}(wa)}{(wa)^r} N_1 e^{jbw} dw \end{aligned} \tag{3.33}$$

$$A\sum_{n=0}^{+\infty} J'_{zn}\int_{-\infty}^{+\infty}\frac{J_{n+s}(wa)}{(wa)^s}\frac{J_{m+r}(wa)}{(wa)^r}M_{11}e^{-j2bw}dw + J''_{zn}\int_{-\infty}^{+\infty}\frac{J_{n+s}(wa)}{(wa)^s}\frac{J_{m+r}(wa)}{(wa)^r}M_{11}dw+$$
$$+ J'_{xn}\int_{-\infty}^{+\infty}\frac{J_{n+p}(wa)}{(wa)^p}\frac{J_{m+r}(wa)}{(wa)^r}M_{12}e^{-j2bw}dw + J''_{xn}\int_{-\infty}^{+\infty}\frac{J_{n+p}(wa)}{(wa)^p}\frac{J_{m+r}(wa)}{(wa)^r}M_{12}dw =$$
$$= -\int_{-\infty}^{+\infty}\frac{J_{m+r}(wa)}{(wa)^r}N_1e^{-jbw}dw \qquad (3.34)$$

The second two expressions are found from the equation (3.26), choosing the signs + and − in the (3.32).

$$A\sum_{n=0}^{+\infty} J'_{zn}\int_{-\infty}^{+\infty}\frac{J_{n+s}(wa)}{(wa)^s}\frac{J_{m+r}(wa)}{(wa)^r}M_{11}dw + J''_{zn}\int_{-\infty}^{+\infty}\frac{J_{n+s}(wa)}{(wa)^s}\frac{J_{m+r}(wa)}{(wa)^r}M_{21}e^{j2bw}dw+$$
$$+ J'_{xn}\int_{-\infty}^{+\infty}\frac{J_{n+p}(wa)}{(wa)^p}\frac{J_{m+r}(wa)}{(wa)^r}M_{22}dw + J''_{xn}\int_{-\infty}^{+\infty}\frac{J_{n+p}(wa)}{(wa)^p}\frac{J_{m+r}(wa)}{(wa)^r}M_{12}e^{j2bw}dw =$$
$$= -\int_{-\infty}^{+\infty}\frac{J_{m+r}(wa)}{(wa)^r}N_2e^{jbw}dw \qquad (3.35)$$

$$A\sum_{n=0}^{+\infty} J'_{zn}\int_{-\infty}^{+\infty}\frac{J_{n+s}(wa)}{(wa)^s}\frac{J_{m+r}(wa)}{(wa)^r}M_{11}e^{-j2bw}dw + J''_{zn}\int_{-\infty}^{+\infty}\frac{J_{n+s}(wa)}{(wa)^s}\frac{J_{m+r}(wa)}{(wa)^r}M_{21}dw+$$
$$+ J'_{xn}\int_{-\infty}^{+\infty}\frac{J_{n+p}(wa)}{(wa)^p}\frac{J_{m+r}(wa)}{(wa)^r}M_{22}e^{-j2bw}dw + J''_{xn}\int_{-\infty}^{+\infty}\frac{J_{n+p}(wa)}{(wa)^p}\frac{J_{m+r}(wa)}{(wa)^r}M_{12}dw =$$
$$= -\int_{-\infty}^{+\infty}\frac{J_{m+r}(wa)}{(wa)^r}N_2e^{-jbw}dw \qquad (3.36)$$

On the parameters s and p the same considerations of the previous section are still valid.

3.3 Numerical results

In this section, some numerical results are presented, always considering as forcing field a wire of current of a plane wave TM and TE polarized. The values used for all the simulation (if not specified differently) are: $a = 1\,mm$ (microstrip half width), $d = 1\,mm$ (dielectric thickness), $\varepsilon_r = 9.2$ (dielectric relative permittivity), $\sigma = 62.8\,MS \cdot m$ (conductibility of the microstrip), $f = 1\,GHz$ (frequency). In case of two microstrips, $b = 2\,mm$ (half distance between the centres of the microstrips).

First of all, a single microstrip is considered and a wire of current is assumed as forcing field. Placing the wire in $\alpha = 0.5mm$ and at different heights, the expansion coefficients and the induced current densities are shown (figures 3.2 and 3.3). The results are also compared with the ones produced by a FEM solver, *Maxwll 2D* by Ansoft.

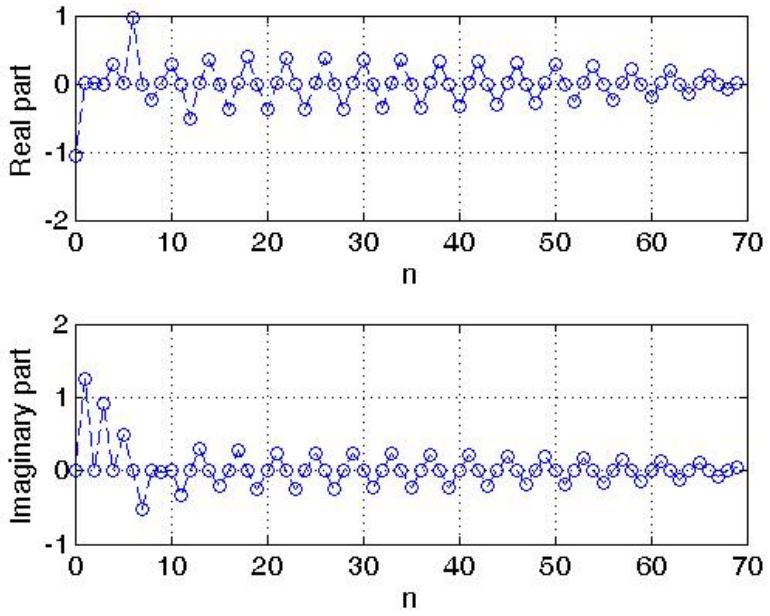

Figure 3.2: Lossy microstrip: Expansion coefficients of current densities induced by a wire

A comparison has to be performed between the induced current density on a perfectly conducting microstrip and a conductive one (figure 3.4).

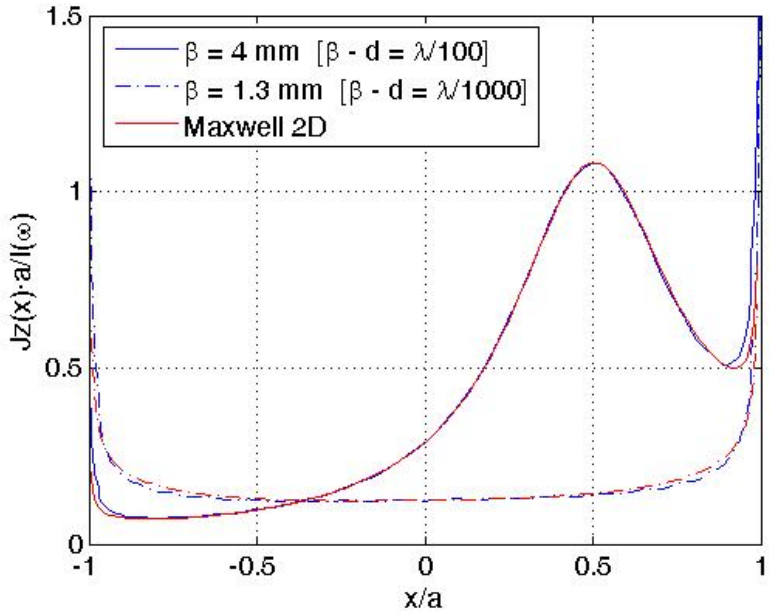

Figure 3.3: Lossy microstrip: Current densities induced by a wire, for different distances, and comparison with a FEM solver

The two curves seem almost to be overlapped, but it needs to keep in mind that the edge behaviour is clearly different. To be sure of that, in figure 3.5 the value of the current density in a corner is plotted as function of the number of expansion coefficients. Of course the current density on the conductive microstrip converges to a finite value, while the current density induced on the lossless microstrip has to diverge.[1] This isn't a trivial difference: to evaluate the conductive losses of the structure, the following integral has to be evaluated:

$$\int_{-a} a|J(x)|^2 dx \tag{3.37}$$

Due to the different edge behaviour, only in the lossy microstrip this integral has a finite value. So the formulation proposed in these chapters can be

[1]To make this simulation, in both the expansions of the current densities has been chosen $s = 1/2$, so the edge behaviour of the current density induced on the lossless microstrip is NOT factorized and visible in the figure. If the edge behaviour is correctly factorized (i.e. $s = 0$), the value of the expansion at the edge is infinite whatever the number of the expansion coefficients may be

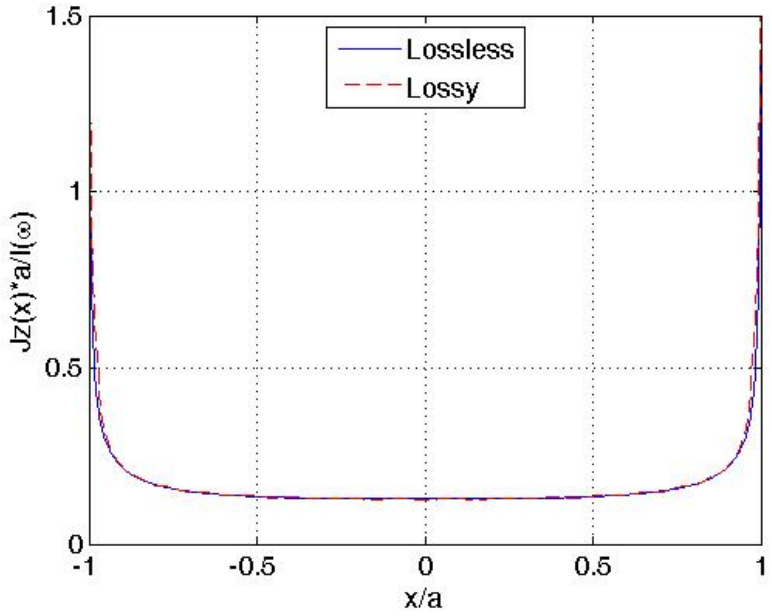

Figure 3.4: Lossy microstrip: Comparison between the current densities induced on a perfectly conducting microstrip and a conductive one

useful to avoid the tricks [6] for the evaluation of the conductive losses.

Then, still using a wire as forcing field, the induced currents are shown for two coupled microstrips (figures 3.6 and 3.7). The wire is always placed in $\alpha = 0.5mm$, so that the two curves are not specular.

Also a plane wave TM polarized is considered as forcing field, in particular when the propagation vector is in the y, z plane ($k_z \neq 0$). In the following figures 3.8 and 3.9, the expansion coefficients and the induced current densities are shown for different incidence angles.

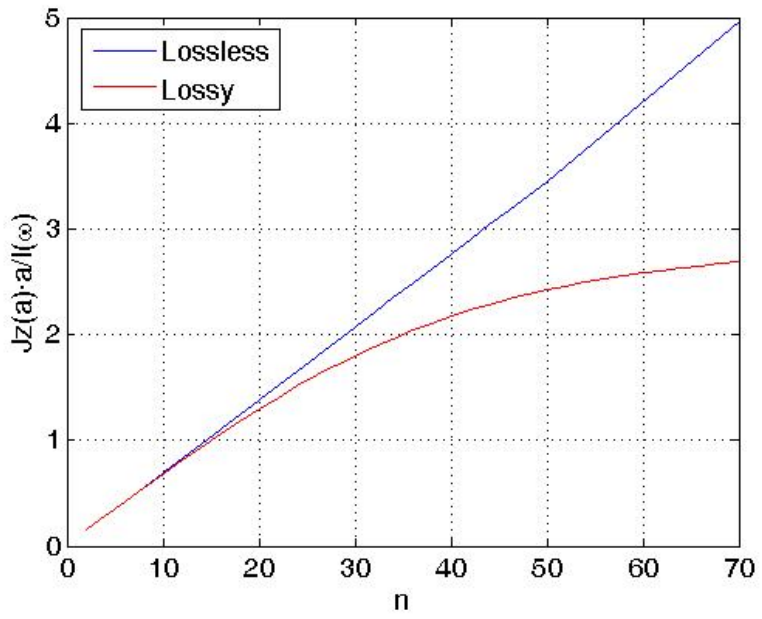

Figure 3.5: Lossy microstrip: Edge value of the current density as function of the number of expansion coefficients

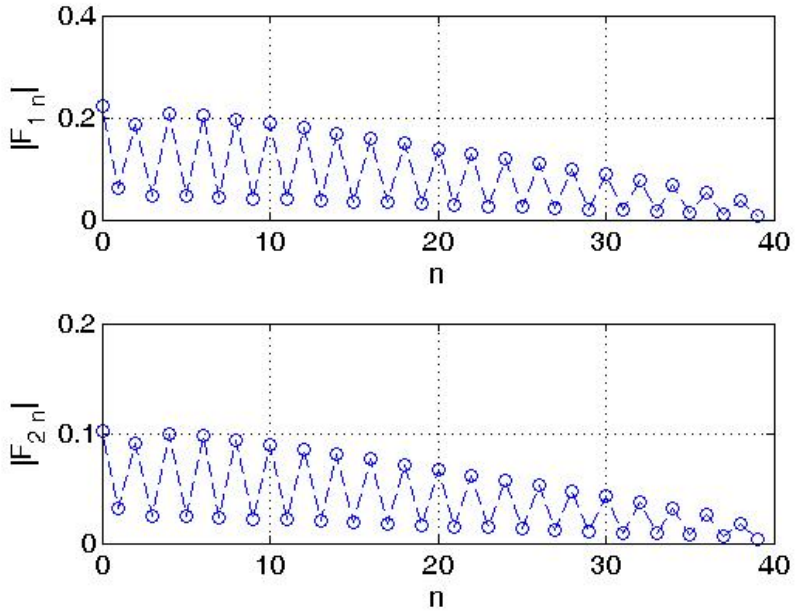

Figure 3.6: Coupled microstrips: Expansion coefficients of current densities induced by a wire

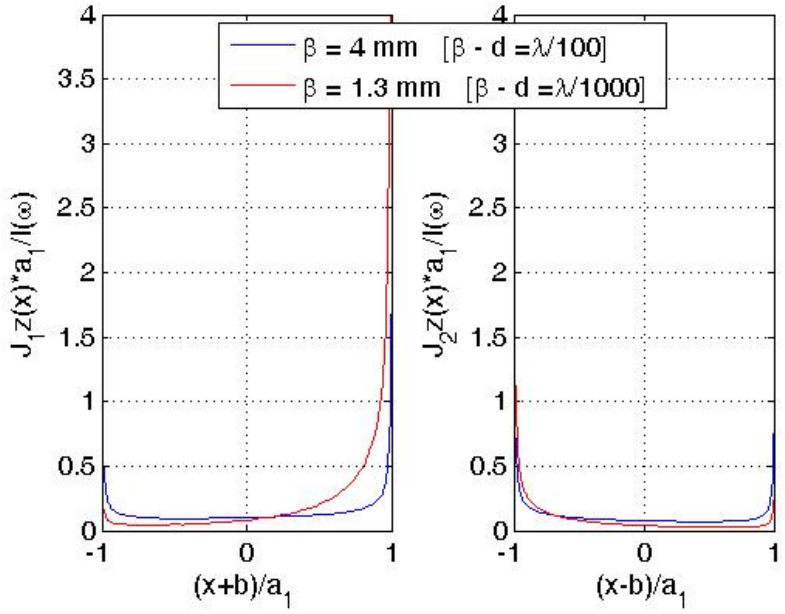

Figure 3.7: Coupled microstrips: Current densities induced by a wire, for different distances

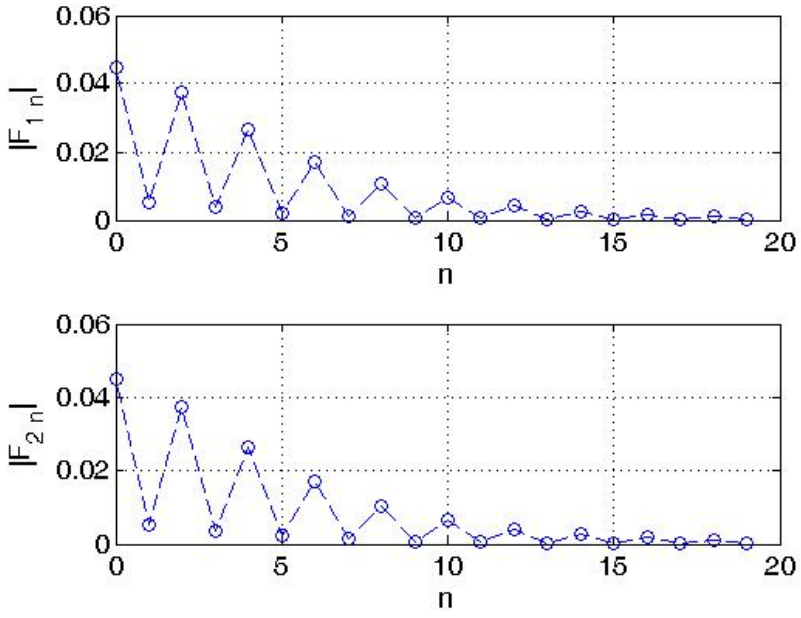

Figure 3.8: Coupled microstrips: Expansion coefficients of current densities induced by a plane wave TM polarized

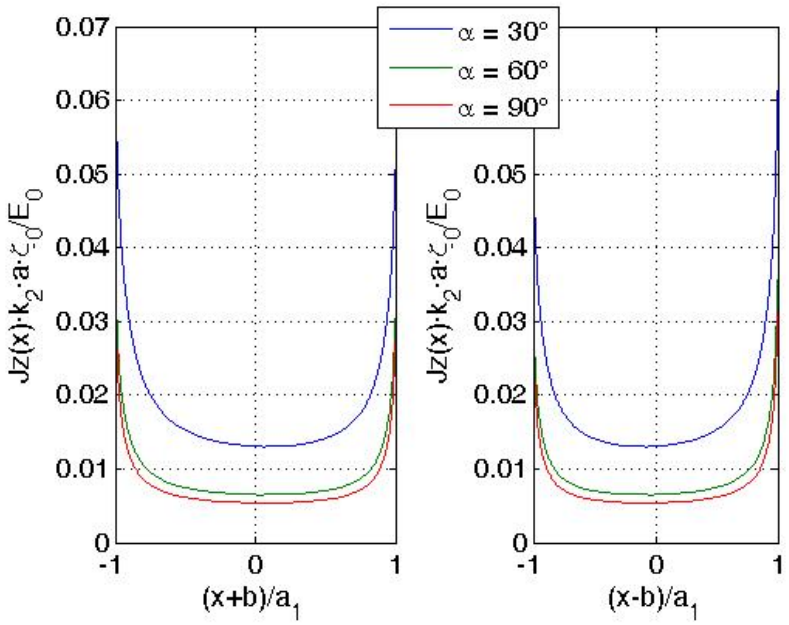

Figure 3.9: Coupled microstrips: Current densities induced by a plane wave TM polarized, for different incidence angles

Chapter 4

Microstrip of finite thickness

4.1 Introduction

In this chapter, a model to analyse microstrips of finite thickness is presented: the current densities induced on the microstrip will be evaluated and a comparison with the microstrip of infinitesimal thickness will be performed.

To simplify the treatment, the microstrip will be supposed to be perfectly conducting. Then, only a wire of current will be assumed as forcing field, so the induced currents will have only a component along the z axis. These two hypotheses reduce the notation and the number of equations, not the difficulty of the problem. However, in the previous chapters it has been shown how these hypotheses can be removed, without besides complicating the treatment.

4.2 Strip of finite thickness in free space

Everybody could imagine that the method used in the previous chapters will also be used to study the microstrip of finite thickness. To arise some doubts, a simpler structure will be quickly studied, only to show how the Neumann series can be used in a different way. The reason of this small digression will be clear as the thick microstrip will be presented.

Anyway, in this section a strip of finite thickness in free space will be examined, whose structure is shown in figure 4.1.

The strip is perfectly conducting, indefinite along the z-direction, has a

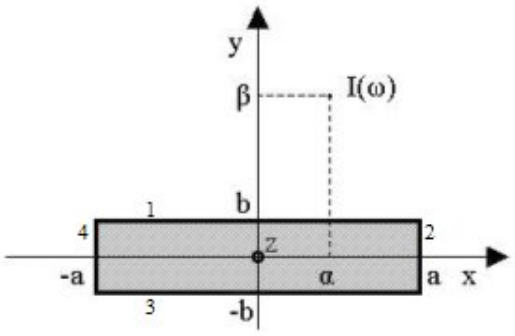

Figure 4.1: Strip of finite thickness in free space

finite width $2a$ and a finite thickness $2b$. A current $I(\omega)$ fluxing in a wire parallel to the z-axis and displaced at (α, β) is assumed as source.

Due to the forcing field, the induced current densities on the strip has only a component along the z axis. So four current densities are defined, namely $J_{z1}(x)$, $J_{z2}(x)$, $J_{z3}(x)$ and $J_{z4}(x)$, according to the numeration of the walls of the strip in figure 4.1.

The electric field produced by an unitary current fluxing along a wire of current placed in (x_0, y_0) is:

$$\vec{E}(x,y) = E(x,y)\hat{z} = -\hat{z}\zeta_0 \frac{k}{4} H_0^{(2)} \left[k\sqrt{(x-x_0)^2 + (y-y_0)^2} \right] \tag{4.1}$$

where $\zeta_0 = \sqrt{\mu_0/\varepsilon_0}$ is the characteristic impedance of the free space.

This expression can be used as Green function to evaluate the electric field

produced by the current densities on the strip:

$$E(x,y) = -\zeta_0 \frac{k}{4} \left\{ \int_{-a}^{a} J_{z1}(x_0) H_0^{(2)} \left[k\sqrt{(x-x_0)^2 + (y-b)^2} \right] dx_0 + \right.$$
$$+ \int_{-a}^{a} J_{z3}(x_0) H_0^{(2)} \left[k\sqrt{(x-x_0)^2 + (y+b)^2} \right] dx_0 +$$
$$+ \int_{-b}^{b} J_{z2}(y_0) H_0^{(2)} \left[k\sqrt{(x-a)^2 + (y-y_0)^2} \right] dy_0 +$$
$$\left. + \int_{-b}^{b} J_{z4}(y_0) H_0^{(2)} \left[k\sqrt{(x+a)^2 + (y-y_0)^2} \right] dy_0 \right\} \qquad (4.2)$$

This field already satisfies the radiation condition, so only the boundary condition on the strip has to be imposed. If $E_0(x,y)$ is the electric forcing field, the boundary condition is:

$$E(x,y) = -E_0(x,y) \qquad \forall (x,y)\ on\ the\ walls\ of\ the\ strip \qquad (4.3)$$

This condition, considering the equation (4.2), is the integral equation that allows to solve the problem. To find a solution, the unknown current densities are expanded in series as follows:

$$J_{z\,i}(x) = \frac{I(\omega)}{a} \frac{1}{\sqrt[3]{1-(x/a)^2}} \sum_{n=0}^{+\infty} F_{i,n} C_n^{1/6} \left(\frac{x}{a} \right) \qquad for\ i = 1,3 \qquad (4.4)$$

$$J_{z\,i}(y) = \frac{I(\omega)}{b} \frac{1}{\sqrt[3]{1-(y/b)^2}} \sum_{n=0}^{+\infty} F_{i,n} C_n^{1/6} \left(\frac{y}{b} \right) \qquad for\ i = 2,4 \qquad (4.5)$$

That expansions are the transforms of Neumann series (see equations (2.79) and (2.82)), as we are working in the spatial domain. In the Neumann series the proper choice is $s = 1/6$ to factorize the right edge behaviour. After that,

the equation (4.3) explicitly becomes:

$$\sum_{n=0}^{+\infty}\left\{F_{1,n}\int_{-a}^{a}\frac{H_0^{(2)}\left[k\sqrt{(x-x_0)^2+(y-b)^2}\right]}{a\sqrt[3]{1-(x_0/a)^2}}C_n^{1/6}\left(\frac{x_0}{a}\right)dx_0+\right.$$
$$F_{2,n}\int_{-b}^{b}\frac{H_0^{(2)}\left[k\sqrt{(x-a)^2+(y-y_0)^2}\right]}{b\sqrt[3]{1-(y_0/b)^2}}C_n^{1/6}\left(\frac{y_0}{b}\right)dy_0+$$
$$F_{3,n}\int_{-a}^{a}\frac{H_0^{(2)}\left[k\sqrt{(x-x_0)^2+(y+b)^2}\right]}{a\sqrt[3]{1-(x_0/a)^2}}C_n^{1/6}\left(\frac{x_0}{a}\right)dx_0+$$
$$\left.F_{4,n}\int_{-b}^{b}\frac{H_0^{(2)}\left[k\sqrt{(x+a)^2+(y-y_0)^2}\right]}{b\sqrt[3]{1-(y_0/b)^2}}C_n^{1/6}\left(\frac{y_0}{b}\right)dy_0\right\}=$$
$$=-H_0^{(2)}\left[k\sqrt{(x-\alpha)^2+(y-\beta)^2}\right] \tag{4.6}$$

That equation has to be verified for every (x, y) belonging to the walls of the strip. To impose this condition, there are different ways. One has been exposed in the previous chapters and it is performed by projecting the equations in the functional space used to represent the unknown density currents. That is simple to do only in the spectral domain, as shown in the previous chapters, but it's easy to find the spatial Fourier transform of the Green function (4.1) and the method could be adopted without effort also for these problems.

Anyway, there is another solution: it's possible to sample the (4.6) in as many points as the number of expansion coefficient desiderated. Also in this way the problem is reduced to an algebraic system.

Some considerations should be done on the two methods. The sampling method leads to an ill-posed problem, so that it could be ineffective if an high number of coefficients has to be calculated. On the other hand it happens only at very high frequencies, at which the projection technique should necessarily be adopted to regularize the problem. The advantage in using the sampling method lies in the numerical calculation of the integrals, that are extended over a finite domain, therefore fast to evaluate. Using the projection method, the integrals are extended over an infinite domain, and therefore slowly converging

and very time consuming. Note that in the spatial domain the projection method is hard to use, except that in some lucky cases.

To solve this problem both the methods could be used, with similar results: we chose to use the sampling method to acquire familiarity with it. Of course the sampling point has to be chosen properly, as they strongly influence the result. On every wall of the strip the number of sampling point is equal to the number of coefficients used to represent the current on that wall. It's well known that, for a polynomial representation, the sampling that produces the minimum quadratic error is in the zeros of the Chebyshev polynomials of first kind [19]. Practically, if N sampling point are required it the interval $[-1, 1]$, the best choice is:

$$T_N(x_k) = 0 \quad \Rightarrow \quad x_k = \cos\left[\frac{(2k+1)}{N}\frac{\pi}{2}\right] \quad for\ k = 0, 1, \ldots, N\text{–}1 \qquad (4.7)$$

Testing different sampling, apart from the benefit on the quadratic error, it has been pleasantly discovered that the expansion coefficients show a faster convergence with respect to the truncation order using the Chebyshev sampling. That is unexpected but desirable because the matrix of the system is not diagonal, so to evaluate such a number of coefficients accurately, always a greater number of coefficients has to be considered.

As a proof of that, in the following figure 4.2, the coefficient $F_{1,2}$ is plotted as function of the truncation order, using an uniform sampling and another as explained above.

Then, just a numerical result is shown to proof the validity of the method. These are the values used for all the simulation: $a = 1\,mm$ (strip half width), $b = 0.1\,mm$ (strip half thickness), $f = 1\,GHz$ (frequency), $\alpha = 0.5\,mm$ and $\beta = 0.5\,mm$ (position of the wire). The expansion coefficients and the induced current densities are shown in the figures 4.3 and 4.4. The results are also compared with the ones produced by *Maxwll 2D*.

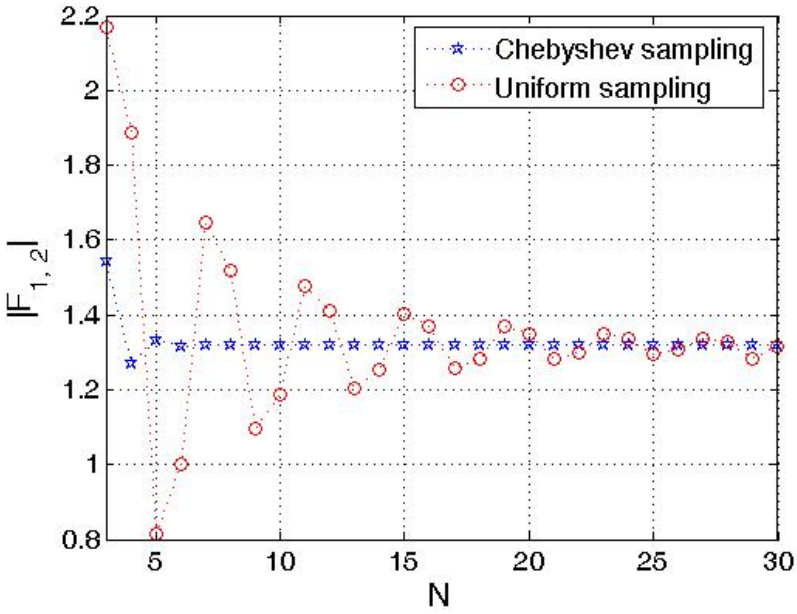

Figure 4.2: Strip in free space: The coefficient $F_{1,2}$ as function of the truncation order, for different sampling

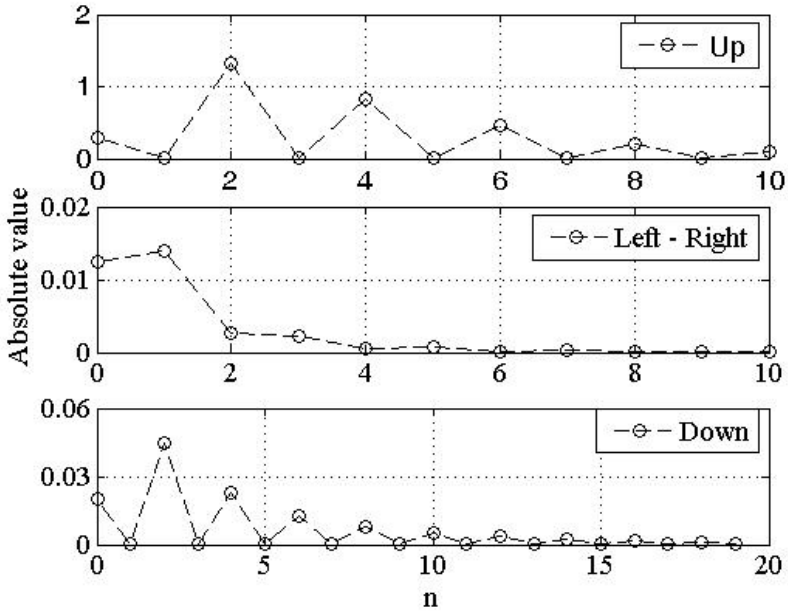

Figure 4.3: Strip in free space: Expansion coefficients of current densities

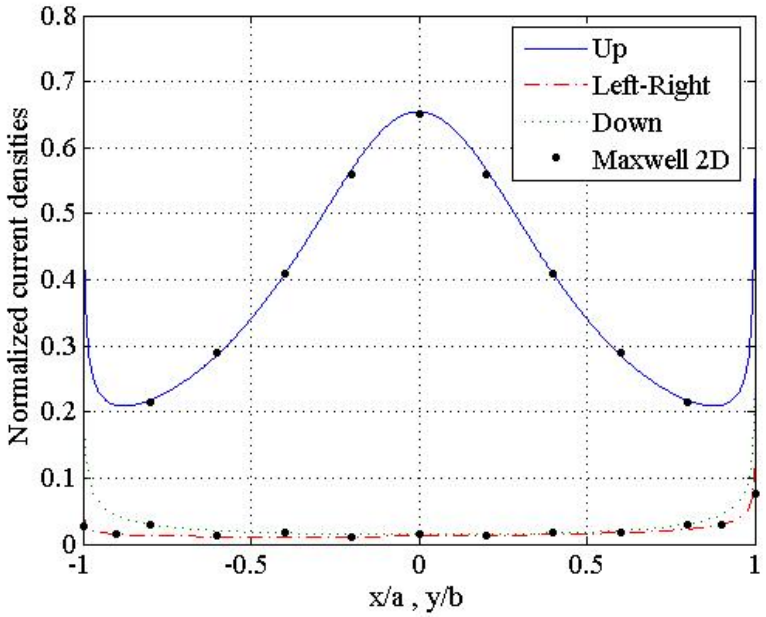

Figure 4.4: Strip in free space: Current densities induced on the walls of the strip and comparison with a FEM solver

4.3 Some problems with the Green function

After the useful digression on the strip in free space, let's go back to the aim of this chapter, a model for a microstrip of finite thickness.

The microstrip is perfectly conducting, indefinite along the z-direction, has a finite width $2a$ and a finite thickness $2b$. The dielectric has thickness d and relative permittivity ε_r. A current $I(\omega)$ fluxing in a wire parallel to the z-axis and displaced at (α, β) is assumed as source (figure 4.5).

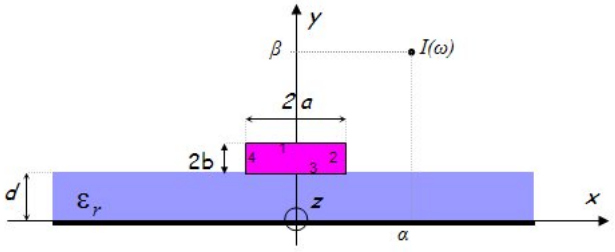

Figure 4.5: Microstrip of finite thickness

Proceeding as in the previous section, the problem can be reduced to the imposition of the boundary condition on the microstrip, that is exactly the equation (4.3). The electric field radiated by the current on the microstrip has to be evaluated. It can be convenient to split the total electric field in four terms, namely $E_1(x,y)$, $E_2(x,y)$, $E_3(x,y)$ and $E_4(x,y)$, each one produced by a single current density. That is to say:

$$E(x,y) = E_1(x,y) + E_2(x,y) + E_3(x,y) + E_4(x,y) \tag{4.8}$$

To evaluate these quantities, the four current densities on the walls of the microstrip, namely $J_{z1}(x)$, $J_{z2}(y)$, $J_{z3}(x)$ and $J_{z4}(y)$, have to be defined. They can be represented as follows:

$$J_{z\,i}(x) = \frac{I(\omega)}{a} \frac{1}{\sqrt[3]{1-(x/a)^2}} \sum_{n=0}^{N} F_{i,n} C_n^{1/6} \left(\frac{x}{a}\right) \qquad for\ i = 1,3 \tag{4.9}$$

$$J_{z\,i}(y) = \frac{I(\omega)}{b} \frac{1}{\sqrt[3]{1-[(y-d-b)/b]^2}} \sum_{n=0}^{N} F_{i,n} C_n^{1/6} \left(\frac{y-d-b}{b}\right) \qquad for\ i = 2,4 \tag{4.10}$$

Then, to evaluate the electric field, the Green function of the problem has to be found. Unfortunately, for such a geometry, it's not possible to express the Green function in the spatial domain. The electric field produced by an unitary current fluxing along a wire of current placed over a dielectric and a ground plane has been derived in appendix 2. This field can be assumed as Green function of the problem and it seems really improbable to find the

transform of such an expression:

$$\tilde{G}(w,y,x0,y0) = \frac{-j\omega\mu\, e^{-jwx_0}}{jA_2 + A_1\cot(A_1d)} \begin{cases} e^{-jA_2(y_0-d)}\frac{sen(A_1y)}{sen(A_1d)} & 0 \le y \le d \\ e^{-jA_2(y_0-d)}\left\{\cos A_2(y-d) + \right. & \\ \left. +\frac{A_1}{A_2}\cot(A_1d)\sin[A_2(y-d)]\right\} & d \le y \le y_0 \\ e^{-jA_2(y-d)}\left\{\cos A_2(y_0-d) + \right. & \\ \left. +\frac{A_1}{A_2}\cot(A_1d)\sin[A_2(y_0-d)]\right\} & y \ge y_0 \end{cases} \tag{4.11}$$

if (x_0, y_0) is the position of the wire.

Being defined the current densities and the Green function, the four components of the electric field can be evaluated. For example, let us study the term $E_1(x,y)$, that is the electric field produced only by the current density $J_{z1}(x)$, using the Green function (4.11). As the boundary condition has to be imposed only on the walls of the microstrip, so always for $d \le y \le 2b$, it's enough to evaluate the electric field in this region. For the quantity $E_1(x,y)$ we have:

$$\begin{aligned} E_1(x,y) &= \int_{-a}^{a} J_{z1}(x_0)\frac{1}{2\pi}\int_{-\infty}^{+\infty}\tilde{G}(w,y,x_0,y_0 = d+2b)\, e^{-jwx}dw\, dx_0 = \\ &= \int_{-a}^{a} J_{z1}(x_0)\frac{1}{2\pi}\int_{-\infty}^{+\infty}(-j\omega\mu)\,\frac{e^{jwx_0}e^{-2jA_2b}}{jA_2 + A_1\cot(A_1d)}\cdot \\ &\quad \cdot\left\{\cos\left[A_2(y-d)\right] + \frac{A_1}{A_2}\cot(A_1d)\sin\left[A_2(y-d)\right]\right\} e^{-jwx}dw\, dx_0 = \\ &= -\frac{j\omega\mu}{2\pi}\int_{-\infty}^{+\infty}\frac{\tilde{J}_{z1}(w)e^{jwx_0}e^{-2jA_2b}}{jA_2 + A_1\cot(A_1d)}\left\{\cos\left[A_2(y-d)\right] + \frac{A_1}{A_2}\cot(A_1d)\sin\left[A_2(y-d)\right]\right\} dw \end{aligned} \tag{4.12}$$

This procedure could be extended also to the other components of the electric field. Then, the total electric field could be evaluated and the boundary condition on the microstrip could be imposed, finding the integral equation that allows to solve the problem. Then, the projection method or the sampling

one could be adopted to solve the equation.

Anyway, following this technique, great computational problems are found. In fact, operating in the spectral domain, all the integrals are extended to an infinite domain. In particular, when the electric field produced by a wall to another *adjacent* is evaluated, the integrals are really slowly convergent. The methods proposed in section 2.5 to accelerate the convergence are unfit for this case and there isn't an efficient technique to this aim. The slow convergence of the integrals is due to the Green function that asymptotically shows an oscillatory behaviour, independently from the representation chosen for the current densities. Of course the problem would be avoided if the Green function could be expressed in the spatial domain. This is still an open problem in literature, and several numerical techniques have been proposed to find an approximation in the spatial domain.

A numerical approximation of the Green function is a delicate operation and has to be avoided if possible: the Green function is the heart of the problem and even a small approximation sometimes could cause the loss of relevant phenomena.

In this case it's possible to avoid an approximation of the Green function. Even if an expression in the spatial domain is unknown, it can be found *partially*. The Green function in the spatial domain is:

$$Gx, y, x_0, y_0 = \frac{1}{2\pi} \int_{-\infty}^{+\infty} \tilde{G}(w, y, x_0, y_0)\, e^{-jwx} dw \tag{4.13}$$

For $y \geq d$, the case of our interest, the Green function can be splitted in two terms. The following expression is valid for both $d \leq y \leq y_0$ and $y \geq y_0$:

$$\begin{aligned} \tilde{G}(w, y, x_0, y_0) = & \frac{-\omega\mu}{2} \left[\frac{e^{jw(x-x_0)}}{A_2} e^{-jA_2|y_0-y|} + \right. \\ & \left. + \frac{e^{jw(x-x_0)}}{A_2} e^{-jA_2(y+y_0-2d)} \frac{jA_2 - A_1 \cot(A_1 d)}{jA_2 + A_1 \cot(A_1 d)} \right] \end{aligned} \tag{4.14}$$

Due to the following integral [22]:

$$\int_{-\infty}^{+\infty} \frac{e^{-j\sqrt{k^2-w^2}|y-y_0|}}{\sqrt{k^2-w^2}} e^{-jwa} dw = \pi H_0^{(2)} \left[k\sqrt{a^2+(y-y_0)^2} \right] \tag{4.15}$$

the transform (4.13) becomes:

$$\begin{aligned} Gx, y, x_0, y_0 = & -\frac{\omega\mu}{4} H_0^{(2)} \left[k_2\sqrt{(x-x_0)^2+(y-y_0)^2} \right] + \\ & - \frac{\omega\mu}{4\pi} \int_{-\infty}^{+\infty} \frac{e^{-jw(x-x_0)}}{A_2} \frac{jA_2 - A_1\cot(A_1 d)}{jA_2 + A_1\cot(A_1 d)} e^{-jA_2(y+y_0-2d)} dw \end{aligned} \tag{4.16}$$

This way to express the Green function has also a physical meaning: the first term, expressed in the spatial domain, is the electric field of a wire placed in (x_0, y_0) in the free space. The second term, that hasn't an analytical transform, represents all the reflection and refractions due to the dielectric and the ground plane.

This expression of the Green function is much more useful, as the electric field $E_1(x, y)$ now becomes:

$$\begin{aligned} E_1(x,y) = & -\frac{\omega\mu}{4} \int_{-a}^{a} J_{z1}(x_0) H_0^{(2)} \left[k_2\sqrt{(x-x_0)^2+(y-d-2b)^2} \right] dx_0 + \\ & - \frac{\omega\mu}{4\pi} \int_{-\infty}^{+\infty} \tilde{J}_{z1}(w) \frac{e^{jwx_0}}{A_2} \frac{jA_2 - A_1\cot(A_1 d)}{jA_2 + A_1\cot(A_1 d)} e^{-jA_2(y-d+2b)} dw \end{aligned} \tag{4.17}$$

Now, using this procedure to calculate the components of the electric field, no problems occur in the evaluation of the electric field produced by a wall to another adjacent. In this case the integral on the compact domain can be evaluated without any effort, while the integral on the infinite domain now is fastly convergent, due to the asymptotic behaviour of the integrand. For example, for the field $E_1(x, y)$ we find the following asymptotic behaviour:

$$\frac{1}{jA_2} \frac{jA_2 - A_1\cot(A_1 d)}{jA_2 + A_1\cot(A_1 d)} e^{-jA_2(y-d+2b)} \quad \sim \quad \frac{e^{-w(y+d+2b)}}{|w|} \tag{4.18}$$

4.4 Formulation of the problem

Following the procedure exposed in the previous section, all the electric fields can be evaluated. In particular, it's easy to find:

$$E_3(x,y) = -\frac{\omega\mu}{4}\int_{-a}^{a} J_{z3}(x_0)H_0^{(2)}\left[k_2\sqrt{(x-x_0)^2+(y-d)^2}\right]dx_0 + \\ -\frac{\omega\mu}{4\pi}\int_{-\infty}^{+\infty}\tilde{J}_{z3}(w)\frac{e^{jwx_0}}{A_2}\frac{jA_2 - A_1\cot(A_1d)}{jA_2 + A_1\cot(A_1d)}e^{-jA_2(y-d)}dw \tag{4.19}$$

For the electric fields $E_2(x,y)$ and $E_4(x,y)$, if it is assumed, as an extension of the (2.26) [1]:

$$\int_{-\infty}^{+\infty} J_{2z}(y)e^{-jA_2y}dy = \int_{d}^{d+2b} J_{2z}(y)e^{-jA_2y}dy = e^{-jA_2(d+b)}\tilde{J}_{2z}[A_2(w)] \tag{4.20}$$

it's simple to find:

$$E_2(x,y) = -\frac{\omega\mu}{4}\int_{d}^{d+2b} J_{z2}(y_0)H_0^{(2)}\left[k_2\sqrt{(x-a)^2+(y-y_0)^2}\right]dy_0 + \\ -\frac{\omega\mu}{4\pi}\int_{-\infty}^{+\infty}\tilde{J}_{z2}(A_2)\frac{e^{-jw(a-x)}}{A_2}\frac{jA_2 - A_1\cot(A_1d)}{jA_2 + A_1\cot(A_1d)}e^{-jA_2(y-d+b)}dw \tag{4.21}$$

$$E_4(x,y) = -\frac{\omega\mu}{4}\int_{d}^{d+2b} J_{z4}(y_0)H_0^{(2)}\left[k_2\sqrt{(x+a)^2+(y-y_0)^2}\right]dy_0 + \\ -\frac{\omega\mu}{4\pi}\int_{-\infty}^{+\infty}\tilde{J}_{z4}(A_2)\frac{e^{jw(a+x)}}{A_2}\frac{jA_2 - A_1\cot(A_1d)}{jA_2 + A_1\cot(A_1d)}e^{-jA_2(y-d+b)}dw \tag{4.22}$$

As the total electric field is known, the boundary condition (4.3) on the

[1] Is this transform correct? For $w > k_2$, the quantity $A_2(w) = \sqrt{k_2^2 - w^2}$ becomes imaginary, so the Fourier transform becomes a Laplace transform. This extension is acceptable as the function to transform, $J_{2z}(y)$, is defined in a compact domain

microstrip can be imposed, obtaining four integral equations, one for each wall of the microstrip. To solve these equations, the Neumann series is used, by means of the expansions (4.9) and (4.10) of the current densities are used. The following representations have also to be used in the spectral domain:

$$\tilde{J}_{z\,i}(w) = I(\omega)\frac{2^{-5/6}\pi}{\Gamma(1/6)}\sum_{n=0}^{+\infty}\frac{\Gamma(1/3+n)}{n!(-j)^n}F_{i,n}\frac{J_{n+1/6}(wa)}{(wa)^{1/6}} \qquad for\ i=1,3 \tag{4.23}$$

$$\tilde{J}_{z\,i}(A_2) = I(\omega)\frac{2^{-5/6}\pi}{\Gamma(1/6)}\sum_{n=0}^{+\infty}\frac{\Gamma(1/3+n)}{n!(-j)^n}F_{i,n}\frac{J_{n+1/6}(b\sqrt{k_2^2-w^2})}{(b\sqrt{k_2^2-w^2})^{1/6}} \qquad for\ i=2,4 \tag{4.24}$$

Note that the series (4.24) is divergent for $w \to \infty$, as the Bessel functions $J_{n+1/6}(\cdot)$ turn into modified Bessel functions $I_{n+1/6}(\cdot)$ for $w > k_2$. Anyway that does not affect the summability of the integrals in the (4.21) and (4.22), due to the presence of $e^{-jA_2(y-d+b)}$.

After that, the system of integral equations can be turned into an algebraic system using the sampling technique described in the previous section.

4.5 Induced current

It may be interesting to perform a comparison between the thin and the thick microstrip. Of course the current densities are unfit for this comparison, while the total induced currents can be useful for this aim. Besides, using the Neumann series, an analytical expression can be found.

This integral can be useful [22]:

$$\int_{-a}^{+a}\left[1-\left(\frac{x}{a}\right)^2\right]^{s-\frac{1}{2}}C_n^s\left(\frac{x}{a}\right)e^{ux}dx = \begin{cases}\frac{a\pi 2^{1-2s}\Gamma(2s)}{\Gamma(s)\Gamma(s+1)} & n=0\\ 0 & n\neq 0\end{cases} \tag{4.25}$$

For the thick microstrip, according to the expansions (4.9) and (4.10), the

total induced current $I_T(\omega)$ is:

$$I_T(\omega) = \int_{-a}^{+a} [J_{z1}(x) + J_{z3}(x)]dx + \int_{d}^{d+2b} [J_{2z}(y) + J_{z4}(y)]\, dy =$$
$$= I(\omega)\frac{2^{2/3}\pi\Gamma(1/3)}{\Gamma(1/6)\Gamma(7/6)}\left[F_{1,0} + F_{2,0} + F_{3,0} + F_{4,0}\right] \tag{4.26}$$

For the thin microstrip, the following limit has to be considered:

$$\lim_{s\to 0}\frac{2^{s-1}\Gamma(2s)}{\Gamma(s)} = 1 \tag{4.27}$$

For this reason, according to the expansion (2.88), the total induced current $I_t(\omega)$ over the thin microstrip is:

$$I_t(\omega) = \int_{-a}^{+a} J_z(x)dy = I(\omega)4F_{z0} \tag{4.28}$$

4.6 Numerical results

In this section, some numerical results are presented. These are the values used for all the simulations (if not specified differently): $a = 1\,mm$ (microstrip half width), $b = a/10 = 0.1mm$ (microstrip half thickness), $d = 1\,mm$ (dielectric thickness), $\varepsilon_r = 9.2$ (dielectric relative permittivity), $\alpha = 0.5\,mm$ and $\beta = 1.5\,mm$ (position of the wire). The expansion coefficients and the induced current densities are shown in the figures 4.6 and 4.7, for a frequency of $100MHz$.

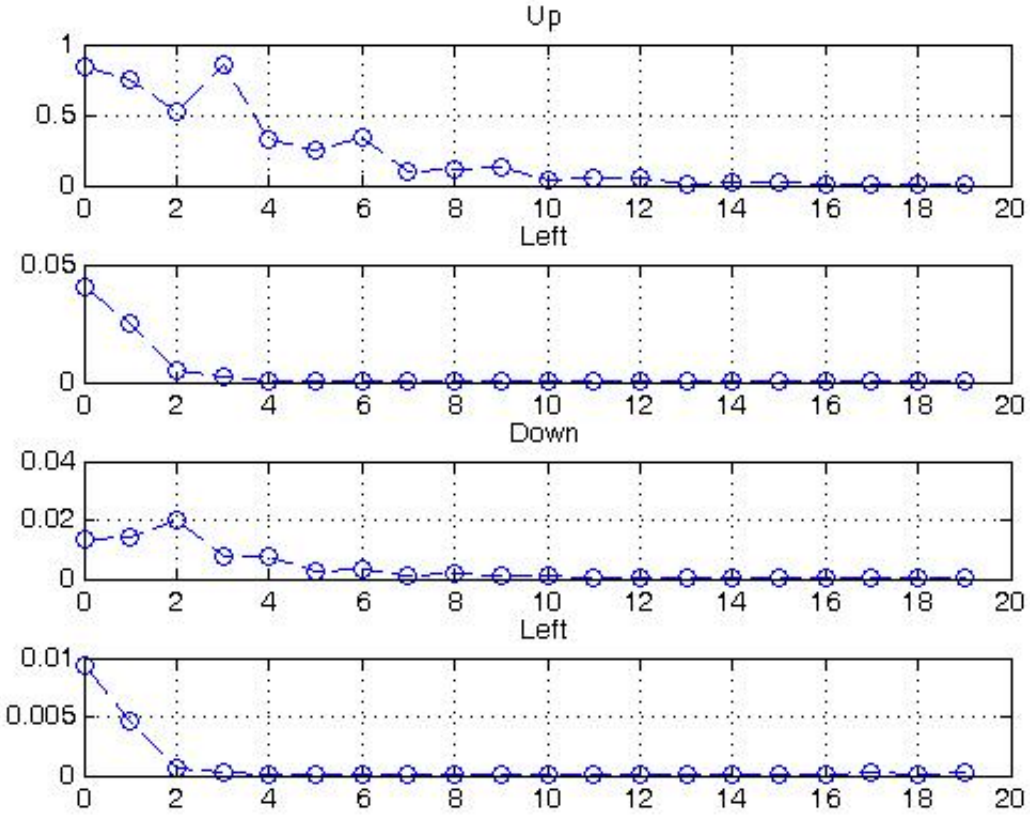

Figure 4.6: Thick microstrip: Expansion coefficients of current densities at 1 GHz

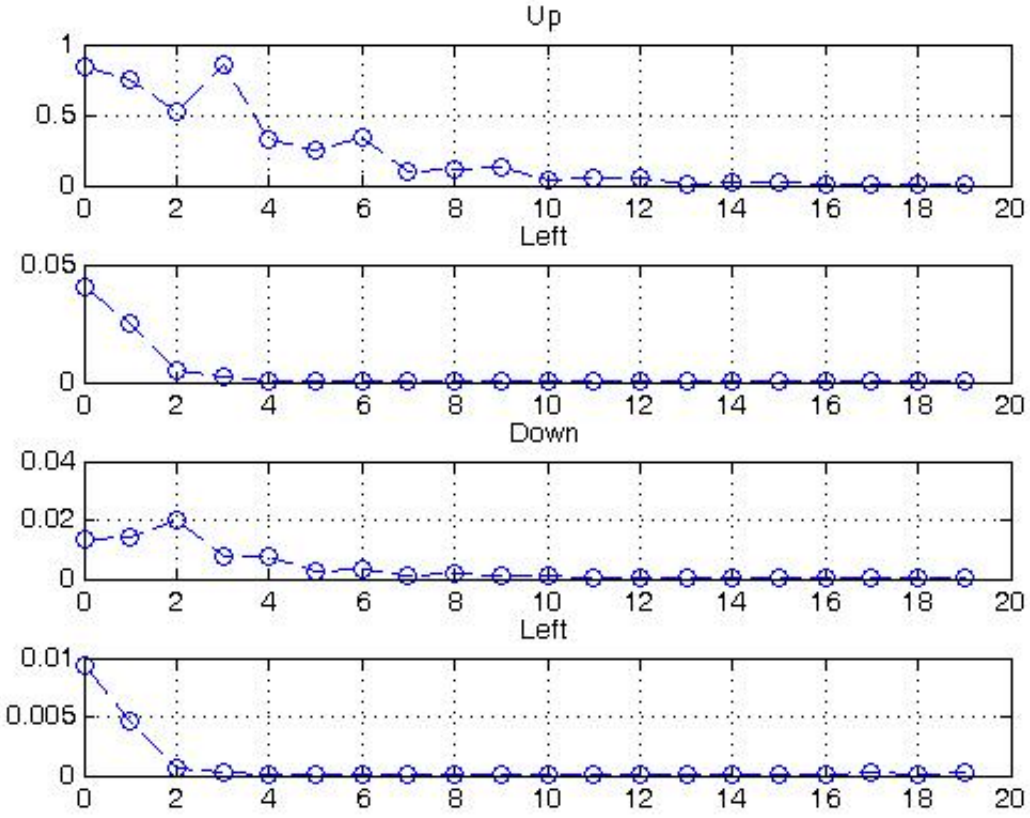

Figure 4.7: Thick microstrip: Current densities induced on the microstrip at 1 GHz.

Chapter 5

Conclusions and outlook

In this thesis, a full-wave model has been introduced for the simulation of microstrip structures. The model allows to examine two remarkable aspects, the finite conductivity and the finite thickness of the conductor, that are generally presented in literature in a doubtful way and however through approximations of various entity. This represents an improvement of the actual models for the simulation and characterization of microstrip structures. In particular, the model proposed to simulate the microstrip of finite thickness uses a rigorous expression of the Green function, while the models actually present in literature only use an approximate expression.

Besides, it has been shown how the proposed method can be easily adapted to study the problem of two coupled microstrips. This technique can also be extended to an arbitrary number of microstrips. Note that the coupling between the microstrips is rigorous, while often in literature it is considered by means of corrective factors.

The presented results can lead to different interesting future developments. From a point of view, it's possible to proceed, from these results, to the extraction of circuital parameters useful for the simulations of more complex structures. Particularly, the model proposed with finite conductivity can allow the evaluation of the resistance of the structure in a more accurate way than how it has been done till now. Another interesting aspect to be easily developed is the improvement of the proposed model, to consider a thick microstrip and of finite conductivity (always Leontovich).

Finally, there are two quests of great interest, that are anyway far to be resolved. The first one is the expression of the Green function in the spatial domain in a rigorous way. The second one is a model for the study of a microstrip of finite thickness and finite conductivity, considering volumetric current densities. These problems are still open, especially the second one, despite the great amount of articles on these arguments.

Appendix A

Properties of some orthogonal polynomials

This appendix doesn't have the pretencion to deeply treat the orthogonal polynomials. An appendix would not be enough, neither this is the purpose of this thesis. Specific texts [21] should be used for this aim. This appendix is simply a brief revision of the fundamental properties of the orthogonal polynomials used in this thesis.

A.1 Orthogonal polynomials

A system of polynomials $f_n(x)$ is orthogonal in the interval $[a, b]$, with respect to a weigh function $w(x)$, if the following equation is satisfied:

$$\int_a^b w(x) f_n(x) f_m(x) dx = 0 \qquad (m \neq n; m, n = 0, 1, 2, \dots) \tag{A.1}$$

The orthogonal polynomials are usually standardized with respect to the following equation:

$$\int_a^b w(x) f_n^2(x) dx = h_n \qquad (n = 0, 1, 2, \dots) \tag{A.2}$$

where h_n is a parameter depending on the type of polynomials.

A.2 Gegenbauer polynomials

The Gegenbauer polynomials $C_n^s(x)$, also said ultraspherical polynomials, are a complete system in $L^2[-1,1]$ and they satisfy the condition (A.1) if the integration interval is $[-1,1]$ and the weigh function is:

$$w(x) = (1-x^2)^{s-\frac{1}{2}} \tag{A.3}$$

About the normalization (A.2), the parameter h_n assumes different values:

$$h_n = \begin{cases} \frac{\pi 2^{1-2s}\Gamma(n+2s)}{n!(n+s)[\Gamma(s)]^2} & s \neq 0 \\ \frac{2\pi}{n^2} & s = 0, n \neq 0 \\ \pi & s = 0, n = 0 \end{cases} \tag{A.4}$$

Such polynomials are solutions, for $s < 0.5$ and n integer, of the Gegenbauer differential equation:

$$(1-x^2)y'' - (2s+1)xy' + n(n+2s)y = 0 \tag{A.5}$$

In general, they can be defined through the Jacoby polynomials $P_n^{(\alpha,\beta)}(x)$ as follows:

$$C_n^s(x) = \frac{\Gamma(s+\frac{1}{2})}{\Gamma(2s)} \frac{\Gamma(n+2s)}{\Gamma(n+s+\frac{1}{2})} P_n^{(s-\frac{1}{2},s-\frac{1}{2})}(x) \tag{A.6}$$

$$P_n^{(\alpha,\beta)}(x) = \frac{(-1)^n}{2^n n!}(1-x)^{-\alpha}(1+x)^{-\beta}\frac{d^n}{dx^n}[(1-x)^{\alpha+n}(1+x)^{\beta+n}] \tag{A.7}$$

Another common definition is the following:

$$C_n^s(x) = \frac{1}{\Gamma(s)} \sum_{m=0}^{[n/2]} \frac{(-1)^m \Gamma(s+m-n)(2x)^{n-2m}}{m!(n-2m)!} \tag{A.8}$$

where $[n/2]$ is the integer part of n/2.

The Gegenbauer polynomials are produced by the following generatrix func-

tion:

$$\frac{1}{(1-2xt+t^2)} = \sum_{n=0}^{\infty} C_n^s(x)t^n \tag{A.9}$$

The first Gegenbauer polynomials are shown:

$$\begin{aligned} C_0^s(x) &= 1 \\ C_1^s(x) &= 2sx \\ C_2^s(x) &= -s + 2s(1+s)x^2 \\ C_3^s(x) &= -2s(1+s)x + \left(\frac{4}{3}\right) s(1+s)(2+s)x^3 \end{aligned}$$

In general, this recurrence equation can be useful:

$$C_n^s(x) = \frac{1}{n}\left[2(n-1+s)xC_{n-1}^s(x) - (n+2s-2)C_{n-2}^s(x)\right]. \tag{A.10}$$

There are some relevant properties related to the derivates of the Gegenbauer polynomials:

$$\frac{d}{dx}C_n^s(x) = 2sC_{n-1}^{s+1}(x) \tag{A.11}$$

$$\frac{d^k}{dx^k}C_n^s(x) = 2^k\frac{\Gamma(s+k)}{\Gamma(s)}C_{n-k}^{s+k}(x) \tag{A.12}$$

$$nC_n^s(x) = x\frac{d}{dx}\left[C_n^s(x)\right] - \frac{d}{dx}\left[C_{n-1}^s(x)\right] \tag{A.13}$$

$$(n+2s)C_n^s(x) = \frac{d}{dx}\left[C_{n+1}^s(x)\right] - x\frac{d}{dx}\left[C_n^s(x)\right]. \tag{A.14}$$

A.3 Chebyshev polynomials

As the Gegenbauer polynomials, also the Chebyshev polynomials of first kind $T_n(x)$ and second kind $U_n(x)$ are a complete system in $L^2[-1,1]$. They are defined as follows:

$$T_n(x) = \cos(n\arccos x) \tag{A.15}$$

$$U_n(x) = \frac{\sin[(n+1)\arccos x]}{\sin(\arccos x)} \tag{A.16}$$

The functions $T_n(x)$ and $\sqrt{1-x^2}U_n(x)$ are independent solutions of the differential equation:

$$(1-x^2)\frac{d^2y}{dx^2} - x\frac{dy}{dx} + n^2y = 0 \tag{A.17}$$

All the zeros of these polynomials are placed in the interval $[-1, 1]$. Further expressions of the polynomials are:

$$T_n(x) = (-1)^n \frac{\sqrt{1-x^2}}{(2n-1)!!}\frac{d^n}{dx^n}(1-x^2)^{n-\frac{1}{2}} \tag{A.18}$$

$$U_n(x) = (-1)^n \frac{(n+1)}{\sqrt{1-x^2}(2n+1)!!}\frac{d^n}{dx^n}(1-x^2)^{n+\frac{1}{2}} \tag{A.19}$$

The first Chebyshev polynomials are shown:

$$T_0(x) = 1 \qquad U_0(x) = 1 \tag{A.20}$$

$$T_1(x) = x \qquad U_1(x) = 2x \tag{A.21}$$

$$T_2(x) = 2x^2 - 1 \qquad U_2(x) = 4x^2 - 1 \tag{A.22}$$

$$T_3(x) = 4x^3 - 3x \qquad U_3(x) = 8x^3 - 4x \tag{A.23}$$

In particular, there are some special cases:

$$T_n(1) = 1 \qquad T_n(-1) = (-1)^n \tag{A.24}$$

$$T_{2n}(0) = (-1)^n \qquad T_{2n+1}(0) = 0 \tag{A.25}$$

$$U_{2n}(0) = 0 \qquad U_{2n+1}(0) = (-1)^n \tag{A.26}$$

In general, these recurrence equations can be useful:

$$T_{n+1}(x) - 2xT_n(x) + T_{n-1}(x) = 0 \tag{A.27}$$

$$U_{n+1}(x) - 2xU_n(x) + U_{n-1}(x) = 0 \tag{A.28}$$

$$T_n(x) = U_n(x) - xU_{n-1}(x) \tag{A.29}$$

$$(1-x^2)U_{n-1}(x) = xT_n(x) - T_{n-1}(x) \tag{A.30}$$

The generating functions of the Chebyshev polynomials $T_n(x)$ e $U_n(x)$ re-

spectively are:

$$\frac{1-t^2}{1-2tx+t^2} = T_0(x) + 2\sum_{k=1}^{\infty} T_k(x)t^k \tag{A.31}$$

$$\frac{1-t^2}{1-2tx+t^2} = \sum_{k=1}^{\infty} U_k(x)t^k \tag{A.32}$$

There is a relevant connection between the Gegenbauer polynomials and the Chebyshef polynomials of first and second kind:

$$\lim_{s\to 0} \Gamma(s) C_n^s(x) = \frac{2}{n} T_n(x) \tag{A.33}$$

$$C_n^{(1)}(x) = U_n(x) \tag{A.34}$$

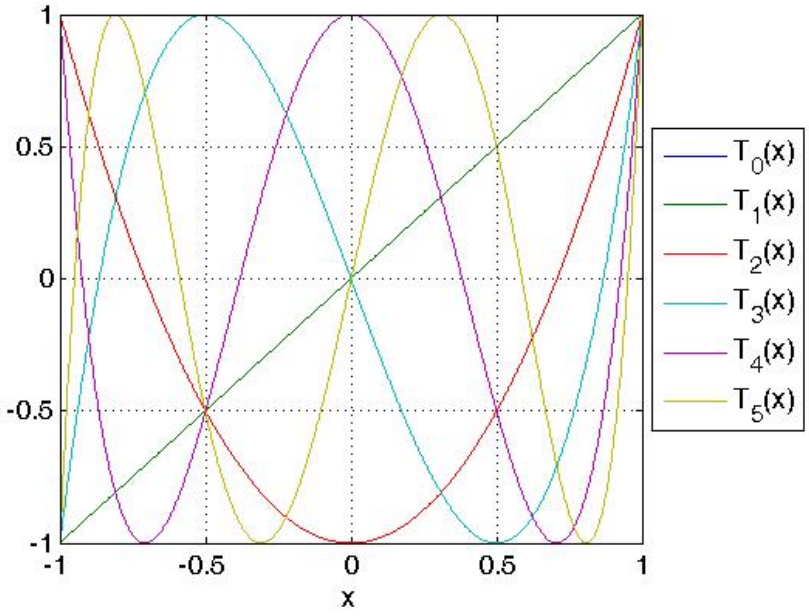

Figure A.1: Chebyshev polynomials of first kind

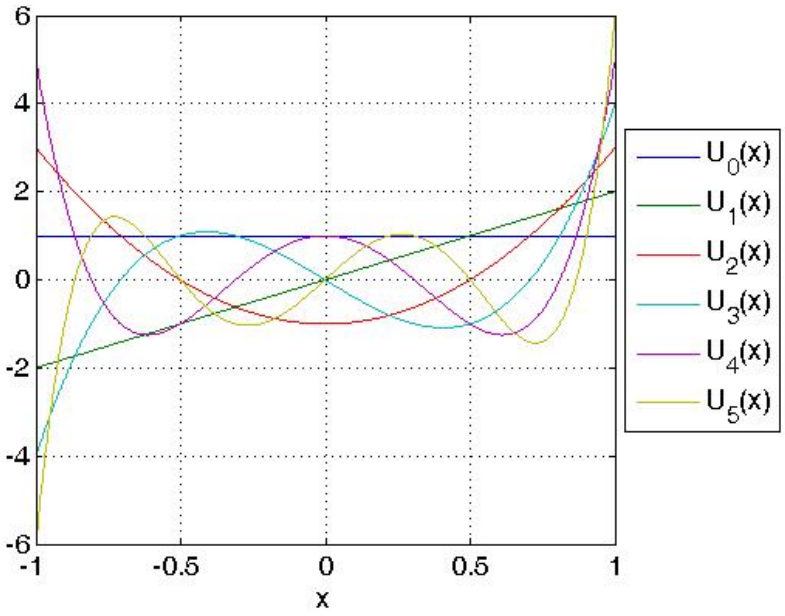

Figure A.2: Chebyshev polynomials of second kind

A.4 Legendre polynomials

The Legendre polynomials, also called Legendre functions of first kind, are solutions of the Legendre differential equation:

$$(1-x^2)\frac{d^2y}{dx^2} - 2x\frac{dy}{dx} + n(n+1)y = 0 \tag{A.35}$$

A particular expression of these polynomials is:

$$\begin{aligned} P_n(x) &= \frac{1}{2^n}\sum_{k=0}^{[n/2]} \frac{(-1)^k(2n-2k)!}{k!(n-k)!(n-2k)!}x^{n-2k} \\ &= \frac{1}{2^n}\sum_{k=0}^{[n/2]} (-1)^k \begin{pmatrix} n \\ k \end{pmatrix} \begin{pmatrix} 2n-2k \\ n \end{pmatrix} x^{n-2k} \end{aligned} \tag{A.36}$$

where $[n/2]$ is the integer part of $n/2$.

The Legendre polynomials are given by the generating function:

$$g(t,x) = (1 - 2xt + t^2)^{-\frac{1}{2}} = \sum_{n=0}^{+\infty} P_n(x)t^n \tag{A.37}$$

From the generating function it's possible to extract a relation useful in many physical problems:

$$(1 - 2xt + t^2)^{-\frac{3}{2}}[1 - t^2] = \sum_{n=0}^{+\infty} (2n+1)P_n(x)t^n \tag{A.38}$$

The first Legendre polynomials are shown:

$$P_0(x) = 1 \tag{A.39}$$

$$P_1(x) = x \tag{A.40}$$

$$P_2(x) = \frac{1}{2}(3x^2 - 1) \tag{A.41}$$

$$P_3(x) = \frac{1}{2}(5x^3 - 3x) \tag{A.42}$$

$$P_4(x) = \frac{1}{8}(35x^4 - 30x^2 + 3) \tag{A.43}$$

In general, these recurrence equations can be useful:

$$(n+1)P_{n+1}(x) - (2n+1)xP_n(x) + nP_{n-1}(x) = 0 \tag{A.44}$$

$$\begin{aligned}(1 - x^2)P_n'(x) &= -nxP_n(x) + nP_{n-1}(x) = \\ &= (n+1)xP_n(x) - (n+1)P_{n+1}(x)\end{aligned} \tag{A.45}$$

The integral of a Legendre polynomial, in the interval $[x, 1]$, for $n \neq 0$, in general is:

$$\int_x^1 P_n(x)dx = \frac{(1 - x^2)}{n(n+1)} \frac{dP_n(x)}{dx} \tag{A.46}$$

In particular, in the interval $[x, 1]$:

$$\int_0^l P_n(x)dx = \frac{P_{n-1}(0) - P_{n+1}(0)}{2n+1} = \begin{cases} 1 & n = 0 \\ 0 & n \neq 0, \textit{even} \\ (-1)^{\frac{n-1}{2}} \frac{n!!}{n(n+1)(n-1)!!} & n \neq 0, \textit{odd} \end{cases} \tag{A.47}$$

There is a relevant connection between the Gegenbauer polynomials and the Legendre polynomials::

$$C_n^{(1/2)}(x) = P_n(x) \tag{A.48}$$

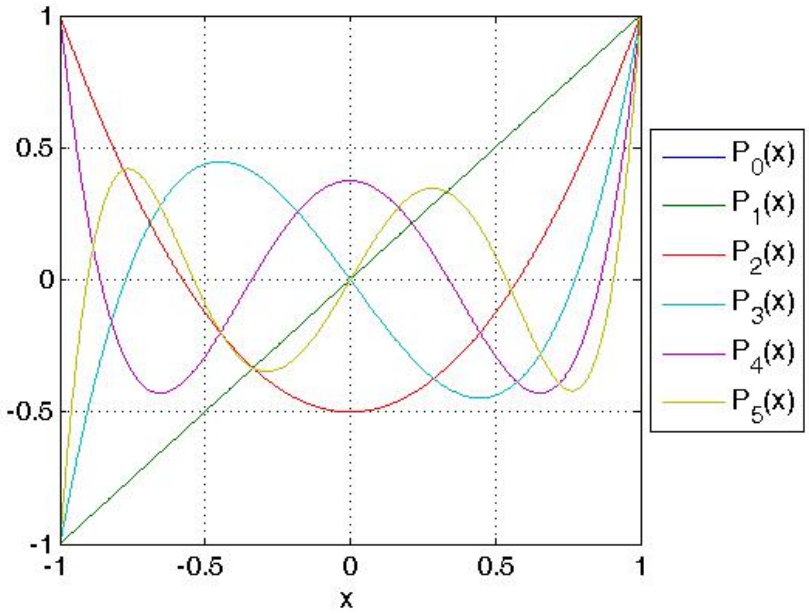

Figure A.3: Legendre polynomials

Appendix B

Canonical sources

The aim of this appendix is to report the expression of the electromagnetic field produced by some canonical sources used in the thesis.

B.1 Wire of current in free space

A wire of current in free space is considered in this section. The value of the current, $i(t)$, is impressed or known. The wire is indefinite along the z axis and it's placed in (α, β) in the x, y plane. The geometry is shown in figure B.1.

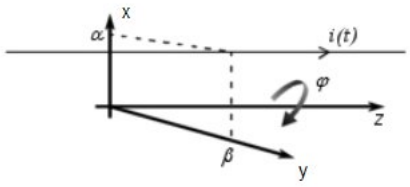

Figure B.1: Wire of current in free space

The current, and so the electromagnetic field, are constant with respect to the z variable. If $I(\omega)$ is the Fourier transform of the current $i(t)$, the electromagnetic field produced by such a structure can be easily found:

$$E_z^0(r) = -\frac{\omega\mu}{4} I(\omega) H_0^{(2)}(kr) \tag{B.1}$$

$$H_\varphi^0(r) = \frac{k}{4j} I(\omega) H_1^{(2)}(kr) \tag{B.2}$$

where $r = \sqrt{(x-\alpha)^2 + (y-\beta)^2}$.

Note that, if $k \to 0$, the well known result is obtained:

$$E_z^0(r) = 0 \tag{B.3}$$

$$H_\varphi^0(r) = \frac{I}{r}\delta(\omega) \tag{B.4}$$

It can also be useful the expression of the electromagnetic field in the spectral domain, coherently with spatial Fourier transform (2.26).

$$\tilde{E}_z^0(w,y) = -\omega\mu\frac{I(\omega)}{2}e^{-jw\alpha}\frac{e^{-jA_2}|y-\beta|}{A_2} \tag{B.5}$$

$$\tilde{H}_x^0(x,y) = -\frac{I(\omega)}{2}e^{-jw\alpha}e^{-jA_2|y-\beta|}sgn(y-\beta) \tag{B.6}$$

$$\tilde{H}_y^0(x,y) = \frac{I(\omega)}{2}we^{-jw\alpha}\frac{e^{-jA_2|y-\beta|}}{A_2} \tag{B.7}$$

B.2 Wire of current over a dielectric substrate

In this section, a wire of current over a dielectric and a ground plane is considered, as shown in figure B.2.

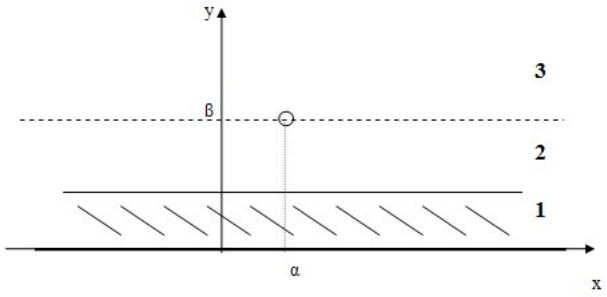

Figure B.2: Wire of current over a dielectric and a ground plane

The space is divided in three zones, identified with 1,2 and 3, that respectively are the dielectric ($0 \leq x \leq d$), the zone between the wire and the dielectric ($d \leq x \leq \beta$) and finally the zone above the wire ($x \geq \beta$).

The electromagnetic field can't be found in the spatial domain explicitly, so it will be found in the spectral domain. Considering the radiation condition

and the presence of the ground plane, following the procedure shown in section 2.2, the electric field in the three zones can be written as follows:

$$\tilde{E}_z^{(1)} = C_1 \sin(A_1 y) \tag{B.8}$$

$$\tilde{E}_z^{(2)} = C_{21} e^{jA_2 y} + C_{22} e^{-jA_2 y} \tag{B.9}$$

$$\tilde{E}_z^{(3)} = C_3 e^{-jA_2 y} \tag{B.10}$$

To determine the coefficients, the boundary conditions have to be imposed. They are the continuity of the tangential component of the electric field along the separation surfaces between the zone 1 and 2 and the zone 2 and 3, the continuity of the tangential component of the magnetic field along the separation surfaces between the zone 1 and 2 and the discontinuity of the tangential component of the magnetic field along the separation surfaces between the zone 2 and 3, due to the wire of current:

$$\begin{cases} C_1 \sin(A_1 d) = C_{21} e^{jA_2 d} + C_{22} e^{-jA_2 d} \\ C_3 e^{-jA_2 \beta} = C_{21} e^{jA_2 \beta} + C_{22} e^{-jA_2 \beta} \\ -A_1 C_1 \cos(A_1 d) + jA_2 [C_{21} e^{jA_2 d} - C_{22} e^{-jA_2 d}] = 0 \\ -[C_{21} e^{jA_2 \beta} - C_{22} e^{-jA_2 \beta}] - C_3 e^{-jA_2 \beta} = \frac{\omega\mu}{A_2} I(\omega) e^{-jw\alpha} \end{cases} \tag{B.11}$$

Solving the system, the constants C can be found, obtaining finally:

$$\tilde{E}_z^{(1)} = -j\omega\mu I(\omega) \frac{e^{-jw\alpha} e^{-jA_2(\beta - d)} \sin(A_1 y)}{jA_2 \sin(A_1 d) + A_1 \cos(A_1 d)} \tag{B.12}$$

$$\begin{aligned} \tilde{E}_z^{(2)} = &-j\omega\mu I(\omega) \frac{e^{-jw\alpha} e^{-jA_2(\beta - d)}}{jA_2 \sin(A_1 d) + A_1 \cos(A_1 d)} \cdot \\ &\cdot \left[\sin(A_1 d) \cos[A_2(y - d)] + \frac{A_1}{A_2} \cos(A_1 d) \sin[A_2(y - d)] \right] \end{aligned} \tag{B.13}$$

$$\begin{aligned} \tilde{E}_z^{(3)} = &-j\omega\mu I(\omega) \frac{e^{-jw\alpha} e^{-jA_2(y - d)}}{jA_2 \sin(A_1 d) + A_1 \cos(A_1 d)} \cdot \\ &\cdot \left[\sin(A_1 d) \cos[A_2(\beta - d)] + \frac{A_1}{A_2} \cos(A_1 d) \sin[A_2(y - d)] \right] \end{aligned} \tag{B.14}$$

B.3 Plane wave TM over a dielectric substrate

In this section, the problem of plane wave TM polarized over a dielectric and a ground plane is examined, considering both the case of the propagation vector in the x, y plane and in the y, z plane, as shown in figure **??** and B.3.

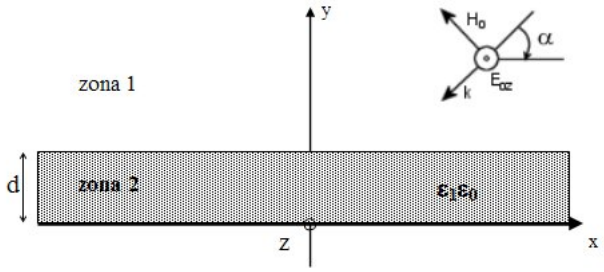

Figure B.3: Plane wave over a dielectric and a ground plane

The space is divided in two zones, identified with 1 and 2, that respectively are the dielectric ($0 \leq x \leq d$) and the zone above it ($x \geq d$).

Let us consider the case of the propagation vector in the x, y ($k_z = 0$). Operating in the spectral domain, if the electric field in the free space is $E_{0z}(x, y) = E_0 e^{jk_2(x\cos\alpha + y\sin\alpha)}$, following the procedure used in the previous section is possible to determine the electric field in the zones 1 and 2:

$$\tilde{E}_{0z}^{(1)}(w, y) = E_0\, e^{jk_2 d\sin\alpha}\delta(w - k_2\cos\alpha)\cdot \tag{B.15}$$
$$\cdot\, \frac{2j\sin\alpha\sin(k_2 y\sqrt{\varepsilon_r - \cos^2\alpha})}{j\sin\alpha\sin(k_2 d\sqrt{\varepsilon_r - \cos^2\alpha}) + \sqrt{\varepsilon_r - \cos^2\alpha}\cos(k_2 d\sqrt{\varepsilon_r - \cos^2\alpha})}$$

$$\tilde{E}_{0z}^{(2)}(w, y) = E_0\, e^{jk_2 d\sin\alpha}\delta(w - k_2\cos\alpha)\cdot \tag{B.16}$$
$$\cdot \left[1 - \frac{\sin\alpha\ \ e^{-jk_2 d\sqrt{\varepsilon_r - \cos^2\alpha}} e^{-k_2(y-d)\sin\alpha}}{j\sin\alpha\sin(k_2 d\sqrt{\varepsilon_r - \cos^2\alpha}) + \sqrt{\varepsilon_r - \cos^2\alpha}\cos(k_2 d\sqrt{\varepsilon_r - \cos^2\alpha})}\right]$$

Then, let us consider the case of the propagation vector in the y, z ($k_z = k_2\cos\alpha$). If the electric field in the free space is $E_{0z}(x, y) = E_0 e^{jk_2(y\sin\alpha + z\cos\alpha)}$,

following the same procedure used above:

$$\tilde{E}_{0z}^{(1)}(w,y) = E_0\, e^{jk_1 d \sin\alpha}\delta(w)\cdot \tag{B.17}$$
$$\cdot\, \frac{2j\sqrt{\varepsilon_r - \cos^2\alpha}\, sen(k_1 y\sqrt{\varepsilon_r - \cos^2\alpha})}{j\sqrt{\varepsilon_r - \cos^2\alpha}\,\sin(k_1 d\sqrt{\varepsilon_r - \cos^2\alpha}) + \varepsilon_r \sin\alpha\cos(k_1 d\sqrt{\varepsilon_r - \cos^2\alpha})}$$

Bibliography

[1] R. E. Collin, *Foundation for microwave engineering*, 2nd Edition, Mc Graw-Hill, Singapore, 1992.

[2] R. F. Harrington, *Time Harmonics Electromagnetic Fields*, McGraw-Hill, London ,1995.

On the microstrips

[3] *Special Issue on "Recent Advances in EMC of Printed Circuit Boards"*, IEEE Transactions On Electromagnetic Compatibility, November 2001.

[4] R. A. Pucel, D. J. Masse, C. P. Hartwig, *Losses in microstrip*, IEEE Transactions On Microwave Theory and Techniques, vol. 16, pp. 343-350, June 1966.

[5] E. Hammerstad, . Jensen, *Accurate Models for Microstrip Computer-Aided Design*, Symposium on Microwave Theory and Techniques, June 1980.

[6] C. L. Holloway, E. F. Kuester, *Edge shape effect and quasi-closed form expressions for conductor loss of microstrip lines*, Radio Science, vol. 29, pp. 539-559, May-June 1994.

[7] D. F. Williams, C. L. Holloway, *Transmission-Line Parameter Approximation for Digital Simulation*, IEEE Transactions On Electromagnetic Compatibility, vol. 43, pp. 466-470, Nov. 2001.

[8] H. Guckel, P. A. Brennan, and I. Palocz, *A parallel-plate waveguide approach to microminiaturized, planar transmission lines for integrated cir-*

cuits, IEEE Transactions on Microwave Theory and Technique, vol. MTT-15, August 1967.

[9] F. Boegelsack, I. Wolff, *Application of a projection method to a mode-matching solution for microstrip lines with finite metalization thickness*, IEEE Transactions on Microwave Theory and Technique, Oct. 1987.

[10] J.D. Morsey, V.I. Okhmatovski, A.C. Cangellaris, *Finite-thickness conductor models for full-wave analysis of interconnects with a fast integral equation method*, IEEE Transactions on Advanced Packaging, February 2004.

On the Neumann series

[11] G. N. Watson, *A treatise on the theory of Bessel functions*, Cambridge University Press, Cambridge 1944.

[12] C. J. Tranter, *Bessel function within some physical applications*, The English University Press, London, 1968.

[13] C. J. Tranter, *A further note on dual integral equation and an application to the diffraction of electromagnetic waves*, Royal Military College of Science, Shrivenham.

[14] F. Erdogan, L. Y. Bahar, *On the solution of simultaneous dual integral equation*, J. Soc. Indust., Appl. Math vol. 12, No 3, September 1964.

[15] K. Eswaran, *On the solution of a class of dual Integral Equations Occuring in Diffraction Problems*, Proc. Royal Society, London, 1990.

[16] I. N. Sneddon, *Mixed Boundary Value Problems in Potential Theory*, North-Holland, Amsterdam, 1996.

Other references

[17] J. Meixner, *The Behaviour of electromagnetic fields at edge*, IEEE Transaction on antennas and propagation, July 1972.

[18] S. Celozzi, G. Panariello, F. Schettino, L. Verolino, *Analysis of the induced currents in finite size PCB round planes*, Electrical Engineering, 2001.

Numerical aids

[19] V. Cominciali, *Analisi numerica*, McGraw-Hill Italia, Milano, 1995.

[20] F. Oberhettinger, L. Badii, *Table of Laplace Transforms*, Springer-Verlag, N.Y., 1972.

[21] M. Abramovitz, I. Stegun, *Handbook of mathematical function*, 9^{th} Edition, Dover, New York, 1972.

[22] I. S. Gradshteyn, I. M. Ryzhik, *Table of Integrals, Series, and Products*, Academic Press, New York, 1980.

List of Figures